DISCLAIMER:

This document does not meet the
current format guidelines of
the Graduate School at
The University of Texas at Austin.

It has been published for
informational use only.

The Thesis Committee for Gabriel Aguilar
Certifies that this is the approved version of the following thesis:

XRF Elemental and Mineralogical Analysis of Core Sample and Well Cuttings in Granite Wash area of Wheeler County, Texas

APPROVED BY
SUPERVISING COMMITTEE:

Supervisor:

William L. Fisher

Harry Rowe

XRF Elemental and Mineralogical Analysis of Core Sample and Well Cuttings in Granite Wash area of Wheeler County, Texas

by

Gabriel Aguilar, B.S.

Thesis

Presented to the Faculty of the Graduate School of

The University of Texas at Austin

in Partial Fulfillment

of the Requirements

for the Degree of

Master of Science in Energy and Earth Resources

The University of Texas at Austin

December 2014

Dedication

This is dedicated to my mother, Charlotte, who has been my rock and always been there for me.

Acknowledgements

Special thanks to QEP Resources Inc. for allowing me to use their data for my thesis. A massive thank you to Derek Hargrave, James Eddleman, and William May for mentoring me as well as Mark Longman for all of his help and insight.

Abstract

XRF Elemental and Mineralogical Analysis of Core Sample and Well Cuttings in Granite Wash area of Wheeler County, Texas

Gabriel Aguilar, M.S. E.E.R.

The University of Texas at Austin, 2014

Supervisor: William L. Fisher

X-Ray Fluorescence (XRF) technology is used in the oil and gas industry to supplement traditionally-acquired well data and to assess mineralogical variability in a non-destructive manner. The application and usefulness of this technology permits many smaller oil and gas companies to spend limited research funds on other areas besides expensive and labor-intensive NMR/SEM/XRD testing. This paper demonstrates XRF technology used for a mineralogical study of the Granite Wash area in Wheeler County, Texas. The Granite Wash is 160 miles long and 30 miles wide and is located in Western Oklahoma and the Texas panhandle and is Pennsylvanian (Morrowan) in age. The most productive stratigraphy in this region comes primarily from several detrital washes derived from the Wichita-Amarillo Uplift (Railroad Commission of Texas). The geologic characteristics of this region range from coarse conglomerates to sandstone, shale, and

turbidite sequences and this is reflected in the complexity and heterogeneity of the reservoirs. The XRF datum are correlated to CoreLab analyses of spectral gamma ray and radioactive elements, confirming the interpretation of the composition of sandstones and organic markers in the subsurface. The heavy and radioactive elements are also helpful in assisting the geologic interpretation to indicate possible maximum flooding surfaces and source rocks containing hydrocarbons. This study also confirms the presence of chlorite and carbonate cements which can have significant effects on porosity and permeability and can lead to and more accurate reservoir characterization of future oil and gas wells. The data from the XRF instrument is also able to support the user in interpreting and recognizing drilling muds that have infiltrated formations and altered the chemical composition of the formation rocks. Plots of pyrite *versus* clay content define trends across the different wells and can help build the subsurface geologic understanding. Finally, the similarities in the readouts of the XRF data are compared with BakerHughes' Rockview nuclear magnetic resonance test to confirm elemental composition and the use of this instrument in assessing the mineralogy and lithology of future oil and natural gas reservoirs.

Table of Contents

List of Tables

List of Figures

Chapter 1 Agenda of Thesis

- Chapter 1 provides an outline of the research and conclusions associated with the thesis topic.
- Chapter 2 focuses on the technology of the XRF instrument along with the geology of the Deep Anadarko Basin.
- Chapter 3 discusses the XRF methodology and sampling techniques used in the study.
- Chapter 4 contains the observations of the data and results utilizing CoreLab spectral gamma ray, K, U, and Th readouts of the Kansas City and Lansing formations. It also assesses potential maximum flooding surfaces rich in organic material as well as lithology of the formations. This chapter also summarizes the results of the XRF elemental readouts and organic indicators on the core sample taking a specific look at the Lansing Group and the Kansas City “A” and “D” formations. An assessment is made of the abundance of Fe vs. S indicating pyrite or chlorite in the various wells and also takes a look at the Al vs. K plots indicating clay content in the formations. Finally, the accuracy of the XRF elemental data versus BakerHughes’ Rockview NMR tool and gives a good indication of how this technology can be accurately used in the future.
- Chapter 5 concludes with a brief overview of all results found in the study and recommends future work.

Chapter 2 Methods

INTRODUCTION

The handheld Thermo Scientific Niton XL3t 900 GOLDD series energy-dispersive X-ray fluorescence (ED-XRF) device conducts rapid, on-site quantitative elemental measurements whose data can be interpreted in recognizing bulk mineral composition and rock properties. This instrument can be particularly advantageous in reducing costly laboratory tests conducted on core samples and well cuttings of potential producing oil and natural gas wells. Moreover, its ability to use x-ray energy to quantify elemental composition can help aid the user in geologic understanding and also has a quick transition period from data collection to data analysis. From this data analysis, interpretations can be made regarding geologic history, composition and mineralogy of the Granite Wash study area.

TECHNOLOGY AND APPLICATION OF XRF INSTRUMENT

The technology of the handheld energy-dispersive XRF device must first be addressed to better understand the quantitative data and how it is obtained. This process is a nondestructive test for material composition. An x-ray is emitted from a miniature x-ray tube inside the device which then determines the chemistry of a sample by measuring the spectrum of the characteristic x-ray emitted by the different elements in the sample when it is illuminated by x-rays (Wirth and Barth 2013). Each element present in the sample will produce characteristic x-rays that can be considered a “fingerprint” for that specific element. When the incoming x-ray of a sufficient energy strikes an atom in the sample, it releases a fluorescent x-ray which then frees an electron from one of the atoms inner orbital shells. The atom then regains its stability and fills the vacancy left in the inner orbital shell with an electron from one of the atoms higher energy orbital shells (Wirth and Barth 2013). The electron drops to a lower energy state by releasing a fluorescent x-

ray, and the energy of this x-ray is equal to the specific difference in energy between two quantum states of the electron (Fitton, 1997). Therefore, when a sample is measured using the handheld XRF instrument, every element in the sample emits its own unique fluorescent x-ray energy spectrum. The device is then able to determine the quantity of each element present in the sample by measuring the fluorescent x-rays emitted by the different elements in the sample.

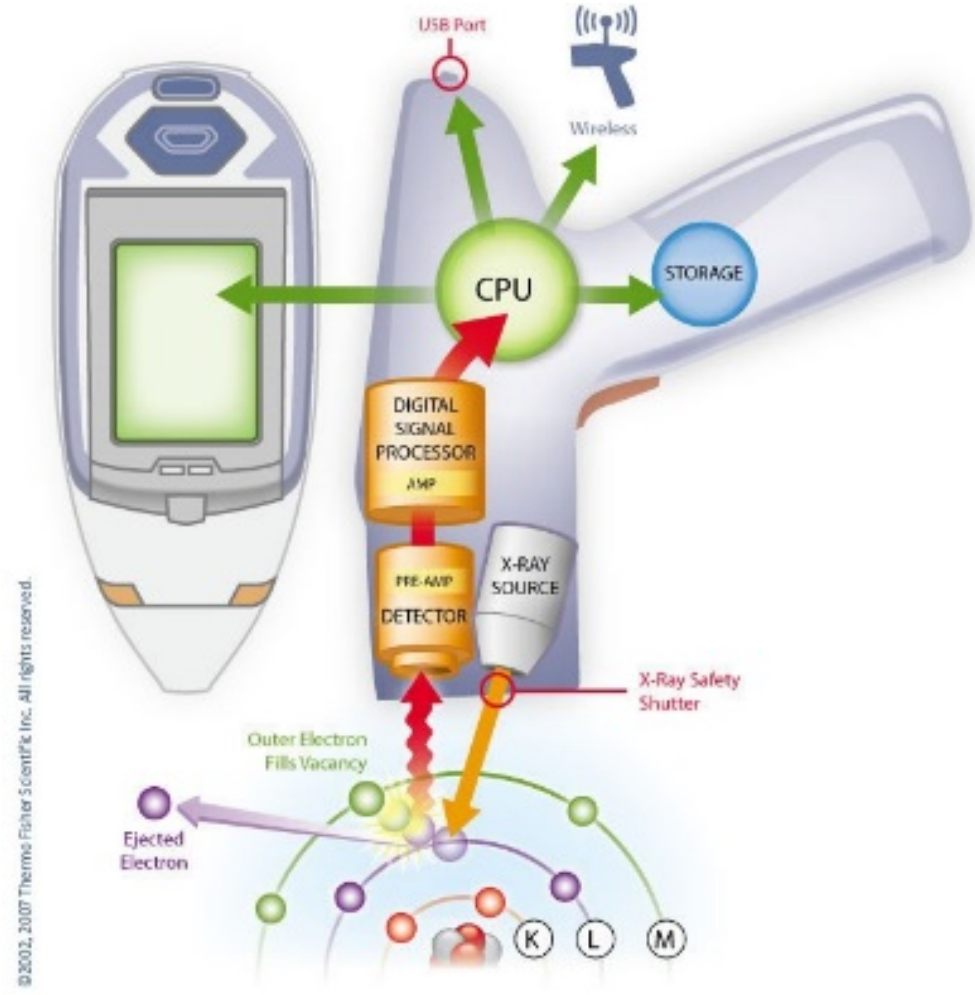

Figure 1: A diagram showing the internal components of the XRF device and the process of emitting x-rays to detect unique elemental signatures.

However, not all of the elements on the periodic table can be read by the device. The introduction of Thermo Scientific's GOLDD technology allows elements below 17 be read by the device. Specifically, these are Mg, Al, Si, P, S, and Cl; all of which hold value in geochemical and petrophysical analysis. Elements lighter than 12 on the periodic table cannot be detected and therefore must be done in a laboratory environment using helium gas purge or a vacuum chamber. However, using the XRF is extremely impractical while using a vacuum purge due to the potential for punctures in the thin window used to seal the instrument from debris and dust. Figure 2 highlights the elements in yellow that can be picked up by the XRF device.

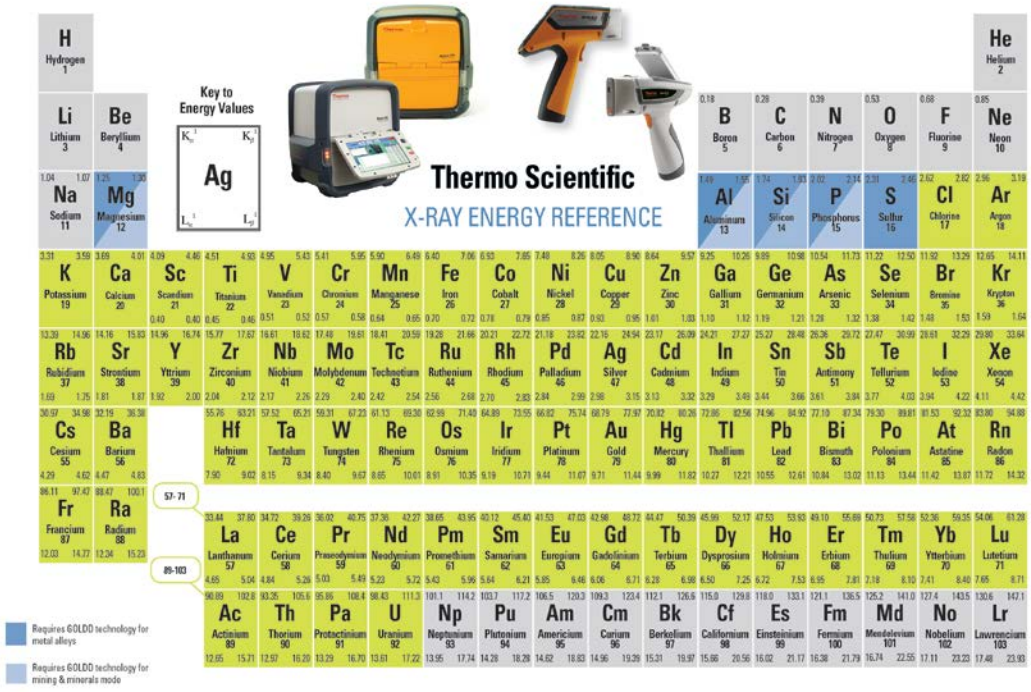

Figure 2: The standard periodic table showing highlighted in yellow and blue the elements that are detected using the XRF device.

The analyzer also contains a software feature that is able to modify which x-ray energies to concentrate on in order to detect either trace or heavy elements and therefore enhance the analysis of certain elements. There are three separate filters that are included in the XRF analyzer and each one can be manually adjusted in the device's touch screen interface to run for different times. The High Filter is used for heavy elements with atomic numbers from 47-56. The Light Filter is used to attenuate the energies that are not of interest and mainly focus on those with atomic numbers less than 17 so that they can be measured more closely. Finally, the Low Filter is primarily used for elements with atomic numbers from 19-24 (K-Cr) (Somarin, 2010). The ability to adjust the analysis times for these three filters can be especially useful when concerned with specific elemental categories and their associations with different petrophysical properties.

The energy dispersive XRF instrument can be used in a wide variety of industries, but geologically it is most commonly used to investigate major and trace elements in either well cuttings or a cored interval. This method is non-destructive and relatively cost-effective and can be used to describe rocks but only after interpretation by the user. It offers quick analysis time and requires minimal sample preparation. XRF analyzers can be used to characterize reservoir properties that influence, but are not limited to, permeability (clays, cement type), porosity (cements), and fracture population (Si content). Element intensities are dependent upon elemental concentration, but they are also influenced by the physical properties of the sample, the sample time, and the energy emitted by the X-ray source (Röhl and Abrams, 2000).

Geology and Production Figures of Deep Anadarko Basin

LOCATION OF STUDY

In conjunction with QEP Resources Inc., the locations and names of the specific wells used in this study will remain undisclosed until production has been fully completed for confidentiality purposes. The location of this research project is located in the northeastern corner of the Texas Panhandle, just north of the Amarillo Uplift in Wheeler County. In Figure 3, the highlighted green area represents Wheeler County and the area shaded in purple is the Granite Wash play.

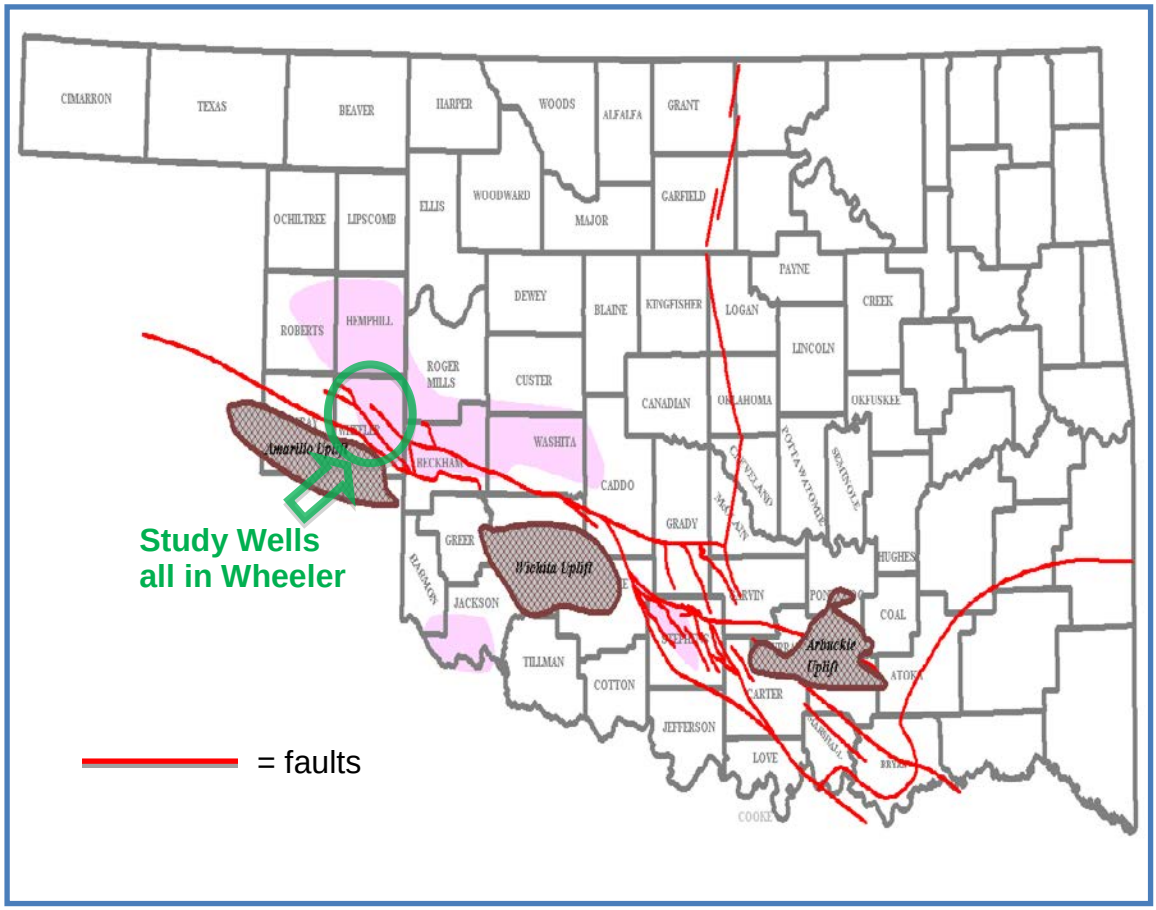

Figure 3: A geologic map of the Texas panhandle (Wheeler Co. in green) and Oklahoma showing the specific location of the study conducted.

The study focuses on six wells that are oriented in a southeast-northwest trend across Wheeler County. The two southeastern-most wells are vertically drilled while the other four are horizontal wells. An 800-foot section of core was recovered from the hydrocarbon bearing zones in one of the wells.

GEOLOGY OF DEEP ANADARKO BASIN

OVERVIEW

In order to better gain an understanding of the Granite Wash study area an overview of the geologic history and setting is presented. The term "Granite Wash" is one that was derived from the weathering of granitic rocks which also contain a close resemblance to the original material (Gelphman, 1960). Specifically, in the Anadarko Basin, this term has become a generally recognized label for the arkosic conglomerate and sandstone that was eroded from the adjacent Amarillo Uplift. Figure 5 is a middle Pennsylvanian paleogeography map, modified from Moore (1979) that shows the deep Anadarko Basin and the surrounding depositional environments and lithologies.

The basin is contained to the east by the Nemaha Uplift and the Arbuckle Mountains and Ardmore basin bound the southeast portion of the study area. To the south the Wichita Mountains and Amarillo Uplift border the Granite Wash and to the west and north, the basin shoals onto a broad shelf with basement depths of less than 5,000-ft (Ball et al., 1991). The study area is updip and to the west of the Anardarko Basin axis (Mitchell, 2011).

LITHOLOGY

To the northeast of the Amarillo Uplift, coarse conglomerates with intermittent amounts of limestone, sandstone, and shale are present. These were deposited by braided-streams, fan-deltas, alluvial fans, proximal turbidite flows and debris flows. More distally to the northeast, however, primarily sandstones and shales that are thought to be deposited as turbidite and debris-flow lobes are observed (Mitchell, 2011). The sediments deposited northeast and proximal to the Amarillo Uplift are primarily arkosic sandstone and conglomerates of Atokan through Virgilian age (Mitchell, 2011). The composition of the Pennsylvanian sandstones and the depositional environment contains detrital minerals and the sandstones reflect the composition of the Precambrian granites and granodiorites that have been exposed in the Amarillo Uplift. Additionally, the arkosic sandstones were deposited in fan deltas that prograded onto a shallow shelf in the southern Anadarko Basin (Dutton 1985).

The height of the Wichita Orogeny occurred during Atokan time uplifted the Amarillo-Wichita Mountains by >10,000-ft in relation to the Anadarko basin axis to the north. The erosion of these mountains provided a distinct conglomeratic wash of granitic sands into the basin. This wash was deposited northward which then combined with felsic sands and shales. In late Pennsylvanian and Desmoinesian time the uplift and faulting began to cease marking the southern portion of the basin. However, the mountains continued to supply quartz sands and granite wash well into Wolfcampian and Permian time as seen in Figure 4. The deposition of granite wash to felsic quartz reached 30 miles northward from the mountain front during the Atokan time period. During the Upper Pennsylvanian a major facies change occurred in which shales and quartz sandstones began to intertwine with the Upper Pennsylvanian shelf carbonates (Ball et al., 1999).

STRUCTURE

Throughout the Paleozoic Era the Anardarko basin was a subsiding tectonic feature. The subsequent faulting that was associated with the Amarillo Uplift helps to define the basin shape at present. The Amarillo Uplift began during early Pennsylvanian (Morrowan time) and continued to uplift into the Lower Permian (Ham et al., 1964; McConnell, 1989). This activity peaked in the Early Pennsylvanian and began to fade by the end of the Permian. The Wichita Orogeny is attributed for the faulting and uplift in the Anadarko Basin and many of the structural characteristics present today in the basin are a result of this event in geologic time (Ball et al., 1999).

The basin contains many anticlinal trends such as the northwest-southeast trending Cordell, Sayre, Mobeetie, and Fort Cobb trends (Wroblewski, 1967). The collision of Gondwana and the Paleozoic North American gave way for the Ouachita and Wichita orogenies in the Early Pennsylvanian with Texas moving north in the direction of the Mid-continent. The Amarillo arch and Wichita Mountains were uplifted and thrust over modern southern Oklahoma. Consequently the loading brought on by the uplifted and overriding north-bound thrust sheets caused new subsidence and this formed the Anadarko Basin. There is general agreement that the Wichita and Ouachita orogenies happened as a result of a collision of crustal plates in the late Paleozoic (Ball et al., 1999). The Late Paleozoic Wichita orogeny is particularly important because it caused the existence of left-lateral strike-slip faulting coupled with folding and thrusting. The majority of the producing structures in the Anadarko Basin appear to be from structural features like these (Ball et al., 1999).

DIAGENESIS

Diagenetic events include the formation of chlorite ooids and precipitation of fibrous submarine Mg-calcite cement which can have an effect on the permeability and porosity

of target formations (Dutton 1985). These events took place in the marine-reworked sandstones in their respective depositional environments. In the reworked sandstones, shallow and early meteoric diagenesis initiated the precipitation of iron-poor calcite spar. Conversely, non-reworked sandstones contain early pore-lining chlorite cement. Finally, moldic porosity created the dissolution of aragonite by fresh meteoric ground water within reworked sandstones. Porosity was then reduced in both reworked and non-reworked fan-delta sandstones because of the precipitation of feldspar, kaolinite, iron-rich calcite, ankerite, and authigenic quartz as burial increased. The final diagenetic events were influenced by the subsequent overlying Permian evaporates. Subsequently this brought sodium-rich fluids and caused albitization of detrital plagioclase and sulfate derived from the evaporites and were precipitated as anhydrite and celestite (Dutton, 1985).

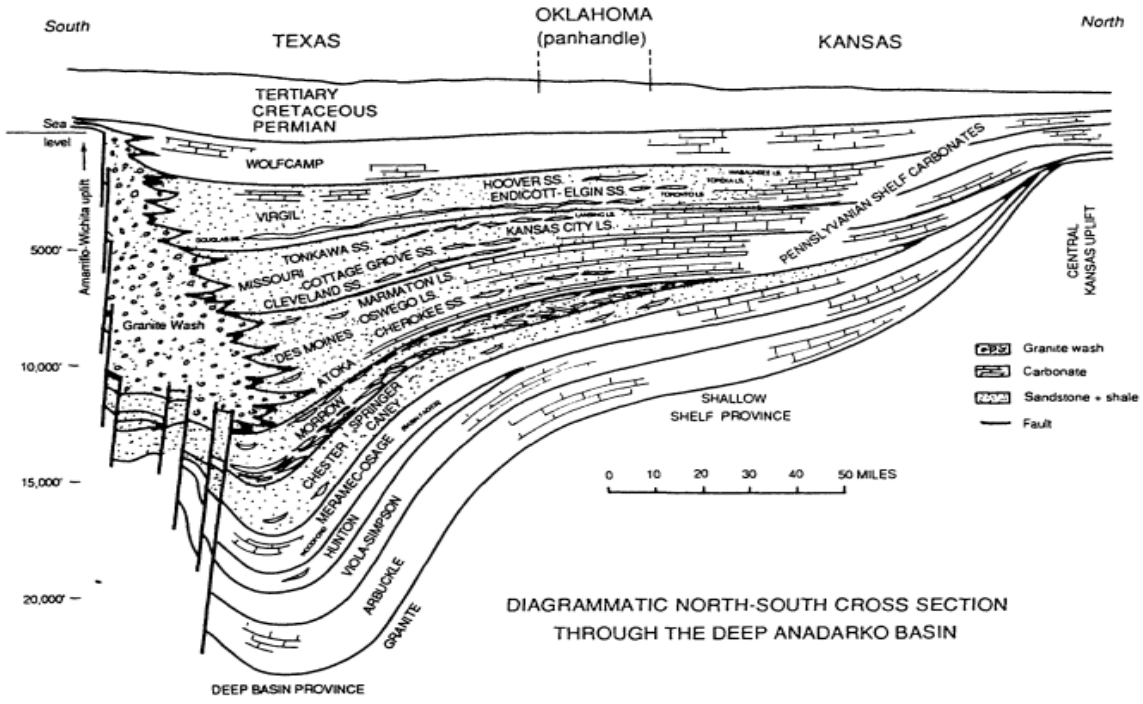

Figure 4: Diagrammatic north-south cross section through the deep Anadarko basin (modified from Hugman and Vidas, 1987)

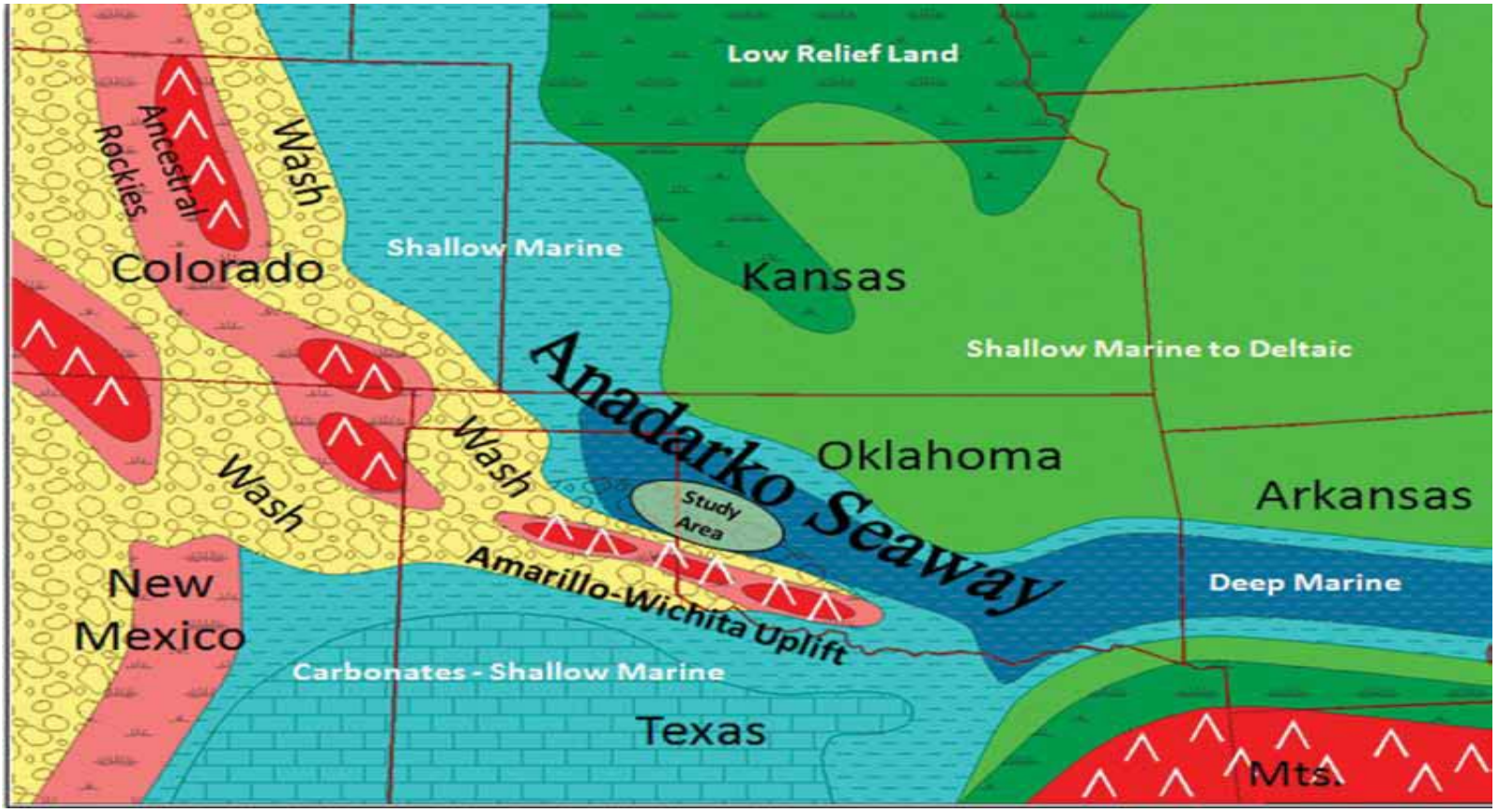

Figure 5: A modified geologic map showing the Granite Wash study area and the geologic setting in which the sediments were deposited in the Pennsylvanian time period. The term "Granite Wash" refers to the weathering of the igneous bedrock in the Amarillo-Wichita Uplift and deposition into the basin to the North (Modified from Moore, 1979)

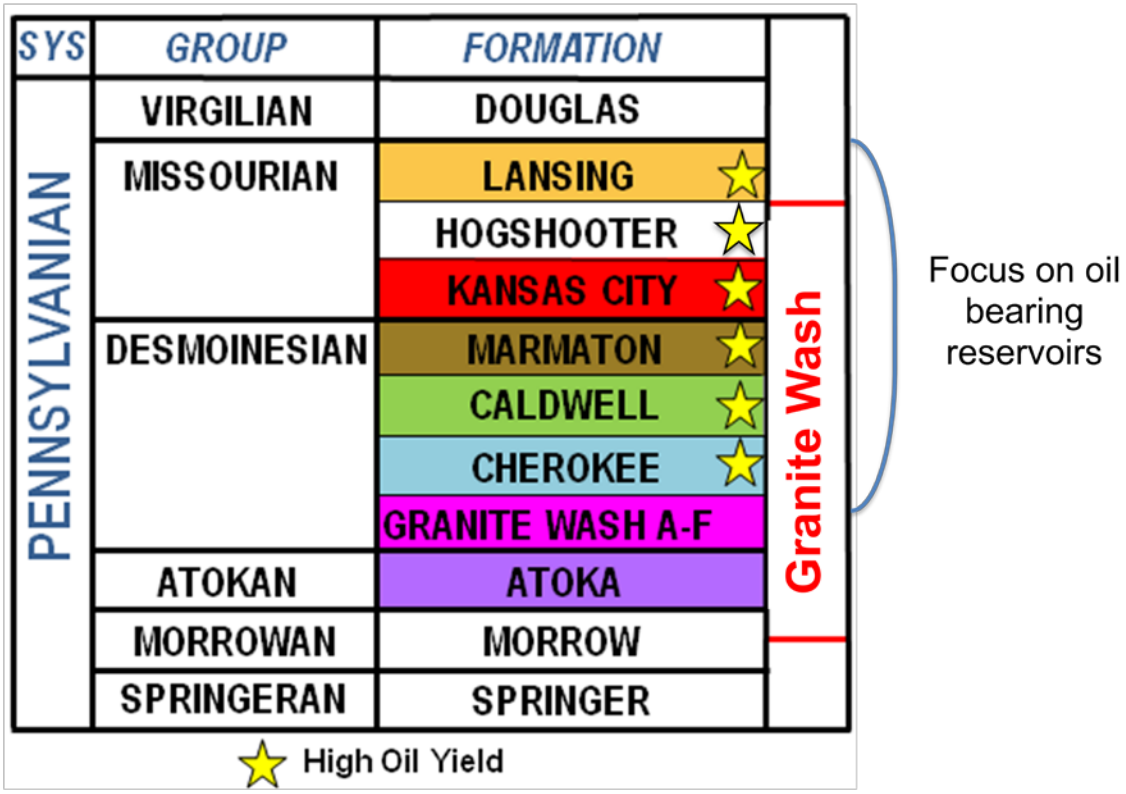

Figure 6: Stratigraphic column of the Pennsylvanian system with specific focus on the oil-bearing reservoir formations of the Lansing, Hogshooter, Kansas City, Marmaton, Caldwell, Cherokee, and Granite Wash.

STRATIGRAPHIC COLUMN

The stratigraphic intervals that are being assessed in this study are shown above in Figure 6. The formations of interest are Pennsylvanian (Missourian and Desmoinesian) in age and marked with a star indicating a proven high oil yield. The Lansing, Hogshooter, Kansas City, Marmaton, Caldwell, and Cherokee units are all classified as interbedded sands and shales while the Granite Wash formation is primarily conglomeritic in nature.

PRODUCTION HISTORY

The Granite Wash study area spans five counties across Texas and Oklahoma and has been producing hydrocarbons ever since the discovery of the Elk City field in Beckham, County, Oklahoma, in 1947. More than 2000 vertical wells have been completed within Granite Wash reservoirs in the five-county area since that time (Mitchell, 2011). As of June 2011, almost 700 horizontal drilling permits have been issued for wells targeting Granite Wash zones with daily production estimated at 41,000 barrels of oil and condensate, 73,500 barrels of natural gas liquids, and 580 million cubic feet of natural gas (Mitchell, 2011).

Vertical drilling has made way for hydraulic fracturing and horizontal drilling in recent times in order to combat the challenges of low permeability and poor recovery efficiency. Large amounts of oil and gas have been left untouched as a result of poor vertical well recovery. The approach recently has been to re-drill existing reservoirs horizontally to maximize economics. Production of this study area has ramped up drastically with this technology and has resulted in higher estimations of recoverable hydrocarbons. With oil prices significantly higher than natural gas prices at this point in time, it makes more economical sense to pursue primarily oil-bearing zones.

Chapter 3 XRF Sampling Technique

INTRODUCTION

The well cuttings that were analyzed in this experiment were provided by QEP Resources Inc., and were promptly washed of formation and drilling fluids after drilling. First, the cuttings were washed with water to remove mud and any water-soluble contaminants followed by another washing with DCM (dichloromethane) solvent. The well cuttings were then placed in individual manila packets that were separated out by depth intervals of 30-feet over the total depth of the well. In horizontally drilled wells, measured depth remained fairly consistent (depending on respective geosteering direction and techniques). Furthermore, a core of over 800-ft was recovered from one of the wells used in the study. Plugs were taken at specified depths in order to assess porosity, oil saturation, and permeability.

The well cuttings were analyzed with the XRF device set up on a stand provided for purposes such as mass sampling. Individual sample cups and an interference-free film were provided as well for well cuttings to be placed and analyzed. The stand includes an area in which to lock in place the XRF device while also providing essential x-ray access to the sample placed in the top of the stand. Lifting the lid on the stand permits the user to place the sample in the top portion of the stand and closing the lid will allow for the sample to be analyzed. After the sample is analyzed, the data are then stored on the XRF device which can then be imported into an Excel spreadsheet for easier workability. This specific model of XRF device also allowed for a real-time video picture to be displayed on the computer screen to ensure that the sample was distributed evenly over the surface of the film. Figure 7 demonstrates a picture of the analysis setup.

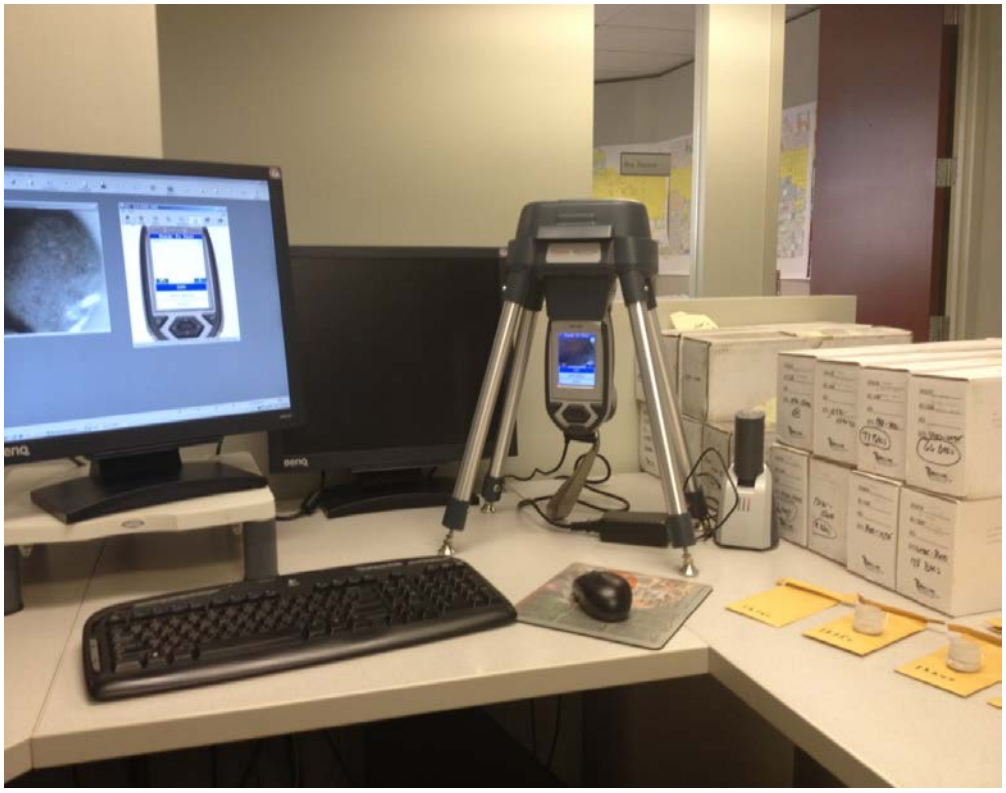

Figure 7: A photograph of the XRF instrument displayed on its stand connected to a computer which was used to collect the data into spreadsheets. On the right side of the photograph sample cups are shown with the well cuttings that were tested beside them.

METHODOLOGY

Both the core sample and well cuttings were analyzed with the XRF device to gain a more complex understanding of mineralogy, elemental chemistry, and chemostratigraphy. For the vertical wells, analyses were done in triplicate for every 30-foot section with the intention of getting the best possible analysis of a very heterogeneous mixture of well cuttings. If only measured once over the interval, the assumption is that not all possible lithological variations in the interval would be represented. In the horizontally drilled wells, one analysis was conducted every 30 feet of

section with the assumption that, once the drillers hit the target section, it remained homogenous throughout the 30-feet. One analysis was taken every 1 foot in the vertically drilled cored interval. Because of the drastic changes in lithology found through the cored interval, the sampling interval was chosen as a starting point. It was not uncommon for the cored interval to contain large rounded igneous clasts so precautions were taken to ensure that the analysis remained in the matrix of the rock. These large clasts were noted in a field notebook and sampled individually later. This cored interval was taken as a reference for the XRF cuttings from other wells.

A total sample time of 75 seconds was chosen based on a study examining the best sample times to detect both trace and heavy elements with the XRF device; 15 seconds was allotted for both the high and low filters whilst the light filter received 45 seconds of analysis. Considering the tight time constraints of the internship, this was an ideal sample time.

Chapter 4 Observations and Results

INTRODUCTION

Part of the CoreLab default services include an output of several different tests conducted on the core sample that is sent to the lab. One of the most basic of these tests is the Spectral Core Gamma Unit which offers total gamma ray recorded in API units. The total spectral gamma ray log is then broken down into three of the most common elements in shales and sands. Potassium (%), Uranium (ppm), and Thorium (ppm) logs display each of these radioactive elements and can be extremely useful in reservoir analysis. Using these three element can help track important features of the sands and clays surrounding the well.

Potassium (K)	clays/feldspars/evaporites
Uranium (U)	organic-rich shales
Thorium (Th)	clays

Table 1: A simplified explanation of three of the most common elements found in shales and sands and their respective lithologic equivalents

Potassium is an indicator for feldspars and clays and can also be present in evaporates. Thorium is usually associated with heavy minerals and is a common component of shales. Uranium frequently indicates organic-rich shales and source rocks (Halliburton).

A maximum flooding surface (MFS) is a stratigraphic marker that is recognized as the deepest water facies within a sequence. It separates the transgressive system tract (TST) from the highstand systems tract (HST) and lies at the turnaround from retrogradational to progradational parasequence stacking (Holland, 2008). It generally shows evidence of slow deposition of sediments as well as burrowing, mineralization and fossil

accumulations. Additionally, when interpreted on logs, the shales immediately above the maximum flooding surface display different qualities than other shales and typically can be recognized based on gamma ray, resistivity, and neutron and density logs (Schlumberger). Using these basic geologic theories, an analysis of the Lansing Group will be addressed, followed by the Kansas City Group.

CoreLab Spectral Gamma Ray, K, U, Th (Organic Indicators)

Lansing Group

Figure 8 shows two possible maximum flooding surfaces at both the base of the Lansing "A" and "B" members. The high uranium content in this section can be an indicator of slow deposition of mudstones coupled with the high intensity spike in the spectral gamma ray. Also, the high uranium spikes in the flooding surfaces indicate organic-rich shale markers at this depth. In the gamma ray log a number of cleaning upward sequences in the primarily sandy part of the formation are seen. These "cleaning upward" sequences represent a change in lithology from primarily shales and mudstones coarsening in grain size to sands and are indicative of changing depositional sequences. Focusing on the potassium content in the Lansing "A" formation, the assumption can be made that quartz sandstones are present in this area. Because of the low potassium concentrations we can justify these sandstones not being arkosic in nature.

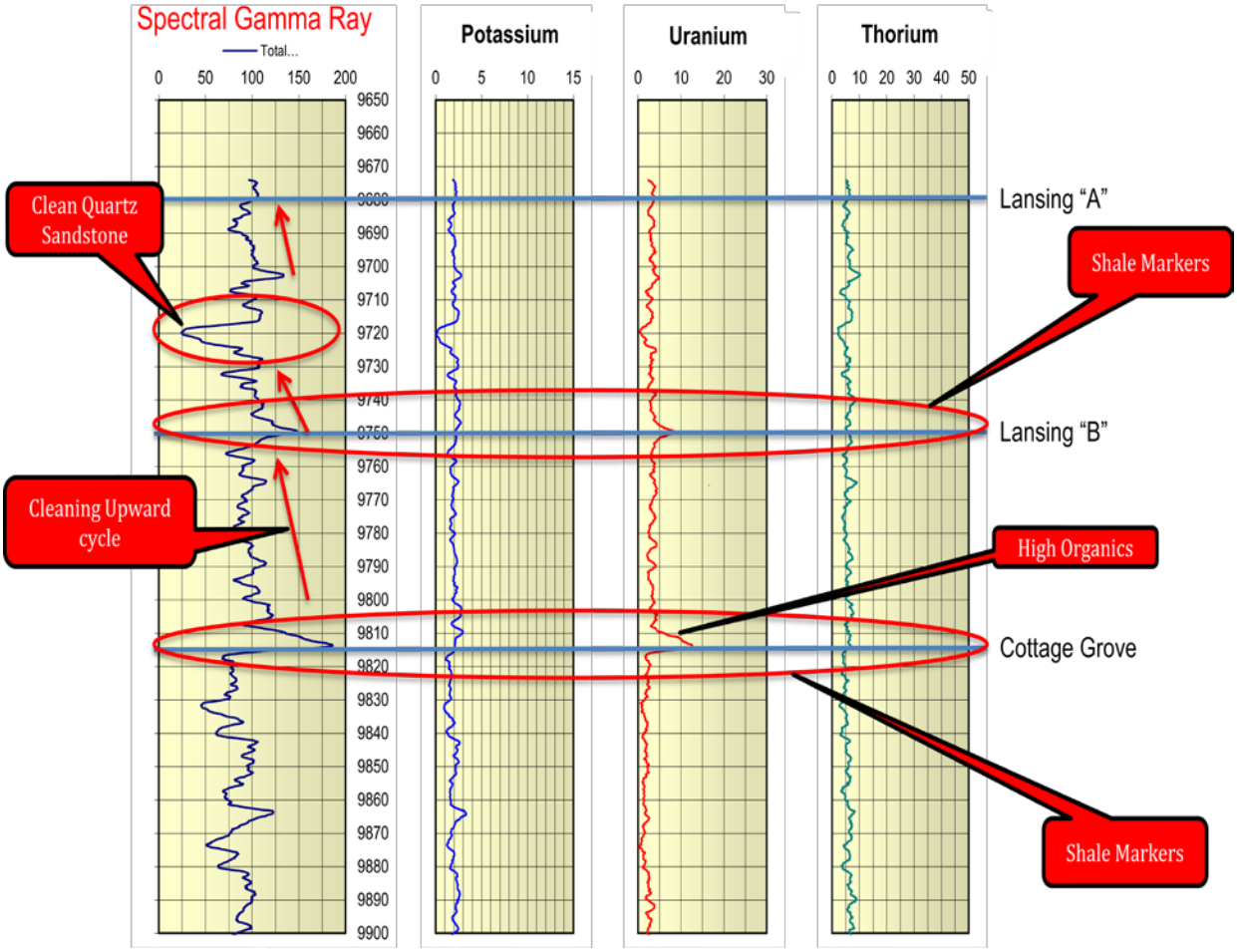

Figure 8: CoreLab standard log of spectral gamma ray, potassium, uranium, and thorium curves of the core sample in the Lansing and Cottage Grove formations.

KANSAS CITY GROUP

In Figure 9, the CoreLab readout is of the Kansas City Group that includes the K, U, Th, and Gamma Ray data. Some observations to be made here are that three more possible maximum flooding surfaces as the bases of the Kansas City "A, B, and D" stratigraphic

members. Again, note the uranium spikes in these intervals which can indicate high organic matter similar to the Lansing Group. Additionally, the spectral gamma ray log contains substantial fluctuation in the data, indicating interbedded sands and shales. While high-organic shales can still be observed in these stratigraphic members, a change in lithology can be noted with the addition of these increasingly sandy intervals.

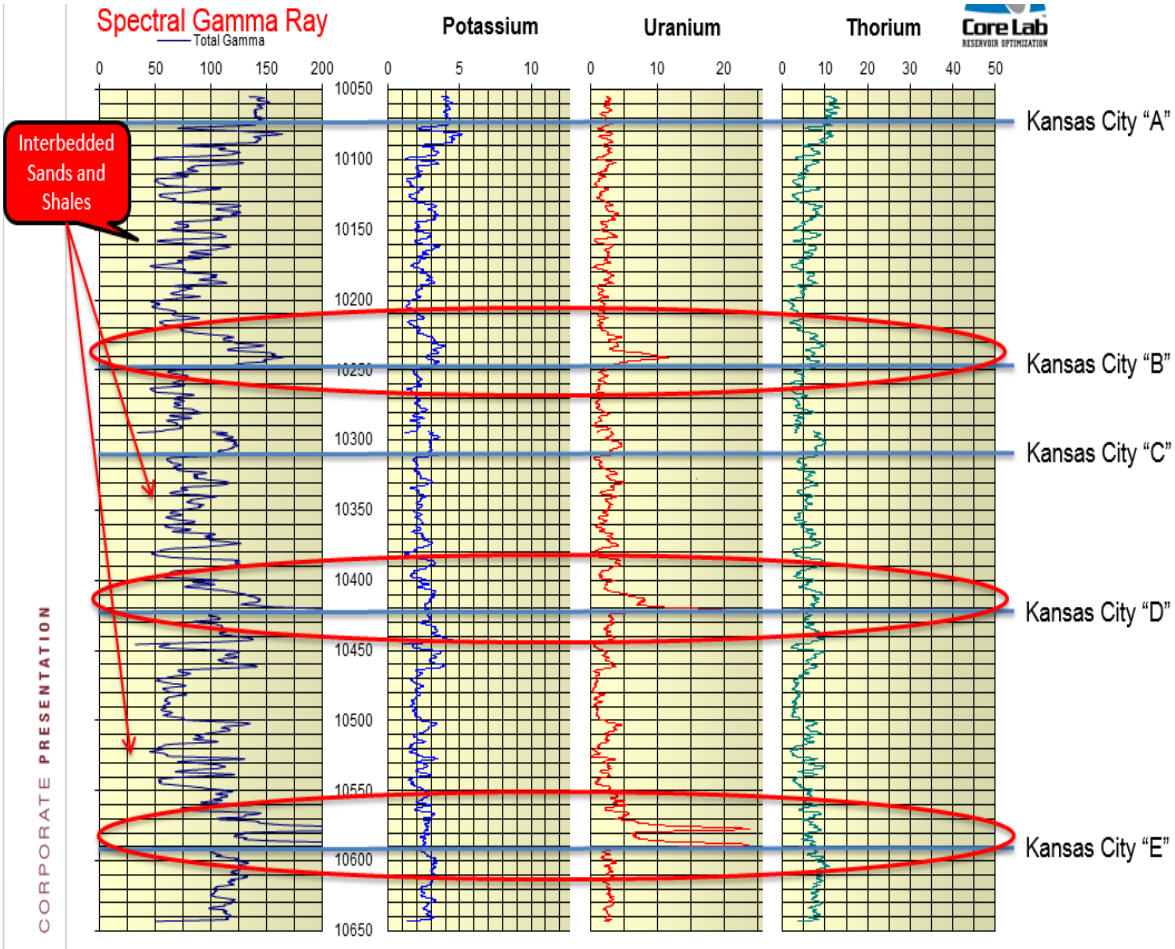

Figure 9: CoreLab standard readout of spectral gamma ray, potassium, uranium, and thorium curves of the core sample in the Kansas City formation.

Chapter 5 XRF Elements Readout (Core Results)

LANSING GROUP (MAJOR XRF ELEMENTS)

Major XRF elements such as Si, Ca, Fe, Al, S, K, Mg, Ti, and Sr are displayed in a log format for easy analysis as seen in Figure 10. These logs were created using a data analytics software program called Spotfire. From these elements, we can infer different mineralogical trends and tendencies, as well as possible depositional environments.

Figure 10 shows the confirmation of the quartz-rich sandstone in the Lansing "A" formation. This is the first validation that the XRF technology is useful in determining mineralogy in a formation solely based on elemental data. In this section it can be demonstrated and is highlighted in red that this sandstone (SiO_2) contains a significant increase in silica content as well as a decrease in potassium to confirm this finding in the CoreLab readout. Additionally, note the increases in both the iron and sulfur content in the base of the Lansing "B" formation indicating the presence of pyrite (FeS_2). This was confirmed when viewing the core under a hand lens.

Also note the high strontium and calcium increases in the Lansing "A" and "B" members that mirror each other in intensity. This can be attributed to some possible carbonate cement but can only be confirmed as so by looking first-hand at the cored interval under magnification. Calcium and strontium are elements that are usually associated with each other when lithified into either calcite or aragonite in marine environments. Both the strontium and calcium are typically derived from the chemistry of the seawater and the carbonate cement is diagenetic in nature. These elements are both naturally occurring in the marine habitat and chemistry as calcium is a major constituent in the earth crust and strontium levels can increase with depth due to acantharians that deposit strontium sulfate skeletons into the rock record (de Villiers et al., 1999). This specific section also

effervesced with hydrochloric acid when testing the core at CoreLab in Houston, TX. It then ceased effervescing after the boundary of the Cottage Grove section. The carbonate cement in this section could be unimportant, but further XRD and SEM tests would need to be conducted to figure out the quantity.

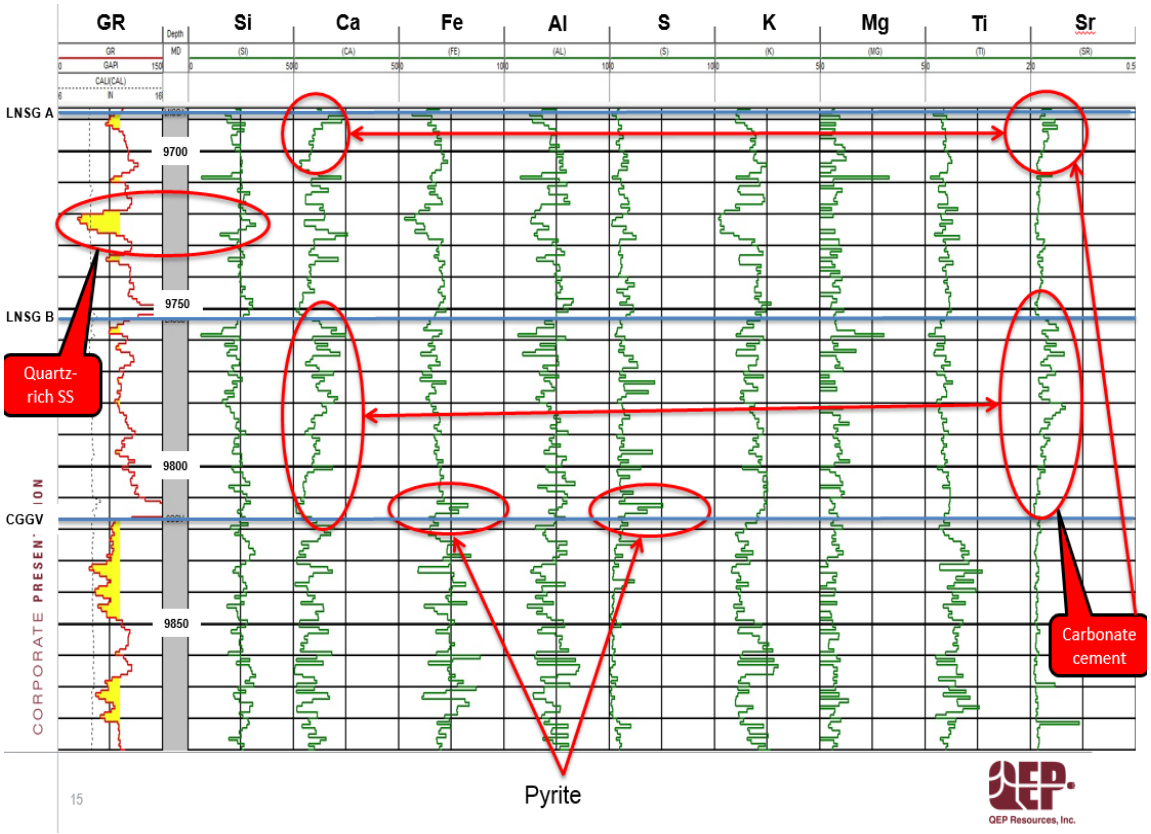

Figure 10: XRF major elemental data being displayed along with the gamma ray curve in the Lansing and Cottage Grove formations.

LANSING GROUP (ORGANIC INDICATORS)

Next, an examination of the organic indictors of the Lansing Group that include V, Cr, U, Se, As, and Mo. Several studies have been conducted on using rock geochemistry to evaluate the state of waters during marine sedimentation, utilizing elements such as these

primarily in black shales (Ross and Bustin, 2009). Moreover, the relationship between Mo, V and Cr can reflect variations in the oxygen content of the seawater during the time of deposition (Smith and Malicse 2010). The elemental logs were created in Spotfire to help create an easy to read interface for the data.

Figure 11 demonstrates an increase in all organic indicators and can be attributed to being a possible source rock in this area. A sharp increase in molybdenum in the XRF data can typically be a characteristic of a quiet sediment starved environment in which this section was deposited in. Molybdenum is an element already present in the seawater and it is precipitated out chemically and can be present in the rock record. This can be an important indicator for depositional environment during this period of geologic time by revealing the seawater and marine conditions.

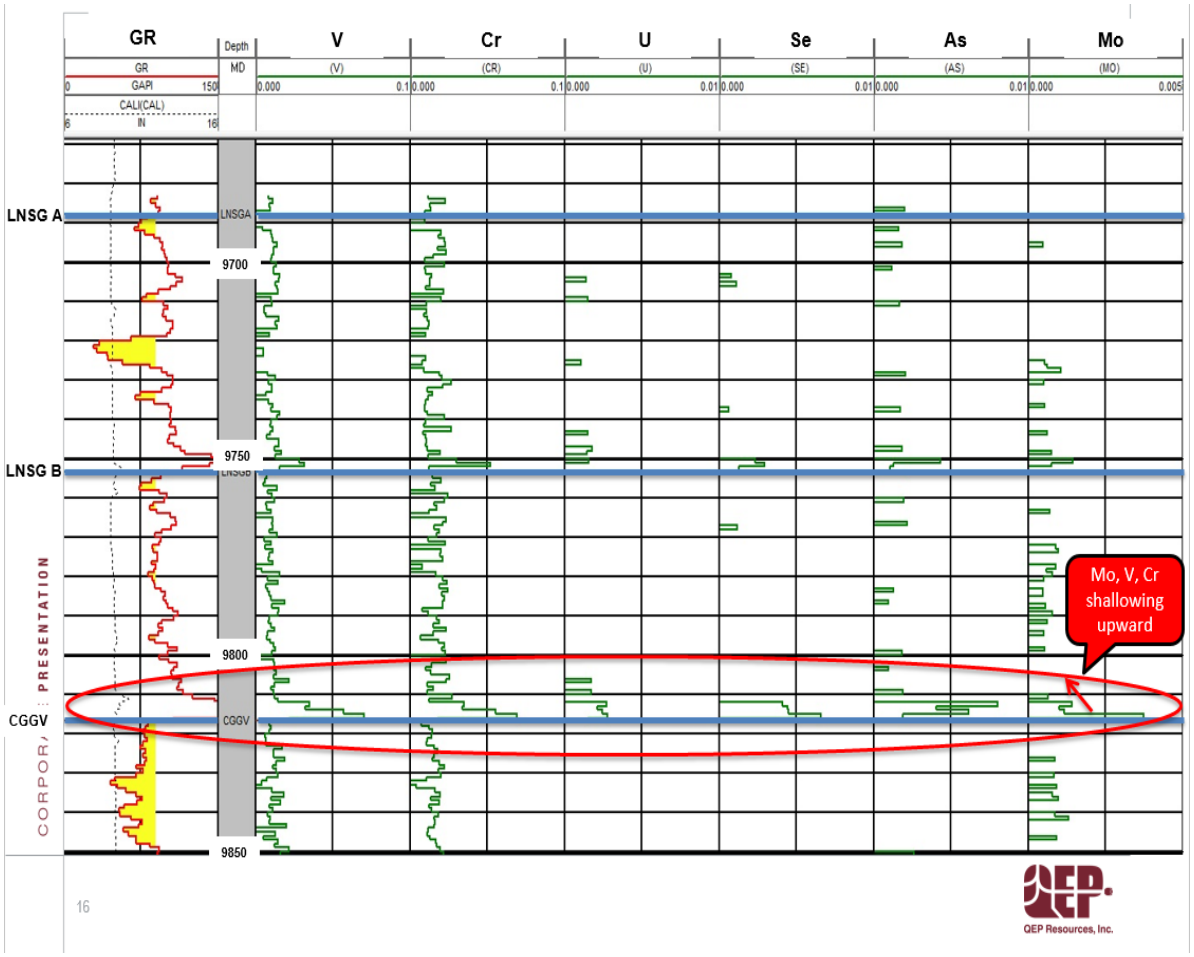

Figure 11: XRF heavy elemental data being shown alongside the gamma ray readout in the Lansing and Cottage Grove formations.

KANSAS CITY GROUP

KANSAS CITY "A"

Next, an assessment of the Kansas City Group and the major XRF elements. In the Kansas City "A" formation is the spike in sulfur from 10,110'-10,120' highlighted in red

in Figure 12. Because there is not a corresponding spike in iron in this section we can assume that it is not pyrite, gypsum or anhydrite. Occasionally during drilling and production it is not uncommon for sulfur to be accompanied with barite. The barite reading for this section has a slight increase that mirrors the sulfur spike in this specific section. There could be possible infiltration of drilling muds into the formation here. The importance of this is that the elemental quantities that the XRF device analyzes is not necessarily entirely formation induced. One very real possibility is that we could encounter drilling induced alterations to the formations with the XRF method.

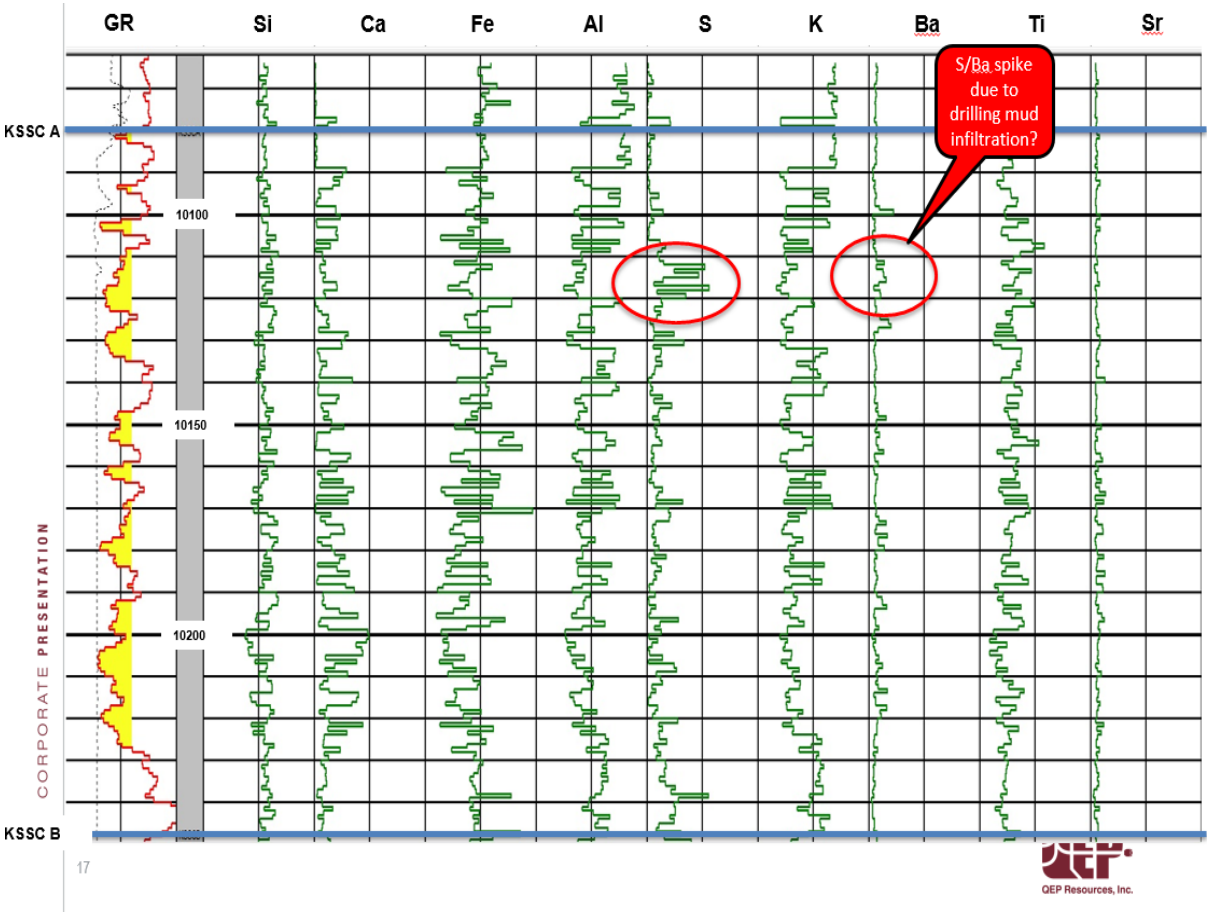

Figure 12: XRF major elemental data displayed alongside gamma ray readouts in the Kansas City "A" formation.

Figure 13 displays blue circles represent plugs that were taken and had tests conducted on them while the yellow circles represent plugs that are to be taken in the future for testing. Testing conducted on the plugs of the core sample at the same depths of 10,110'-10,120' a porosity of 8.5% is observed, which leaves sufficient pore space available for drilling mud infiltration. This porosity value was calculated by using a pressure-transient technique (CoreLab). This reaffirms the hypothesis of infiltration in this area along with the fact that there is 0% oil saturation.

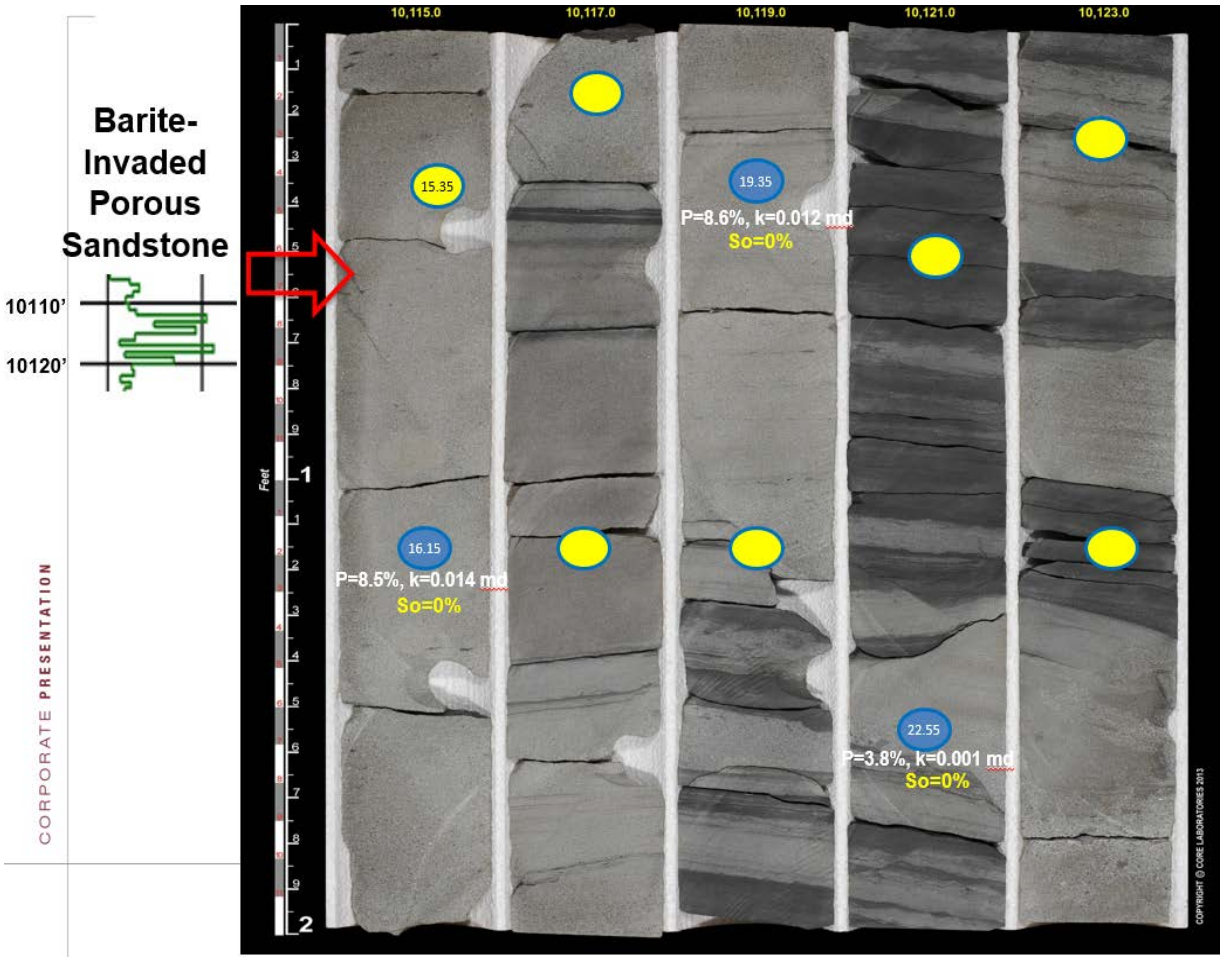

Figure 13: CoreLab photograph of core sample of Kansas City "A" formation to show confirmation of drilling mud infiltration into the formation at depths of 10110'-10120'. Porosity and permeability measurements are also shown where plugs were taken.

Another observation to make on this section is the calcium and strontium relationship observed in Figure 14. Toward the bottom of the Kansas City "A" formation, the strontium is not mirroring the calcium. This is an indication of authigenic calcite cement that is forming in this area. Normally, both strontium and calcium would have precipitated out of the water during deposition in a marine environment and fill the pores but the absence of strontium here indicates that this calcite is not derived from the seawater chemistry (de Villiers et al., 1999). From this we can assume that the calcite cement in this area is authigenic or was formed during sedimentation by either recrystallization or precipitation.

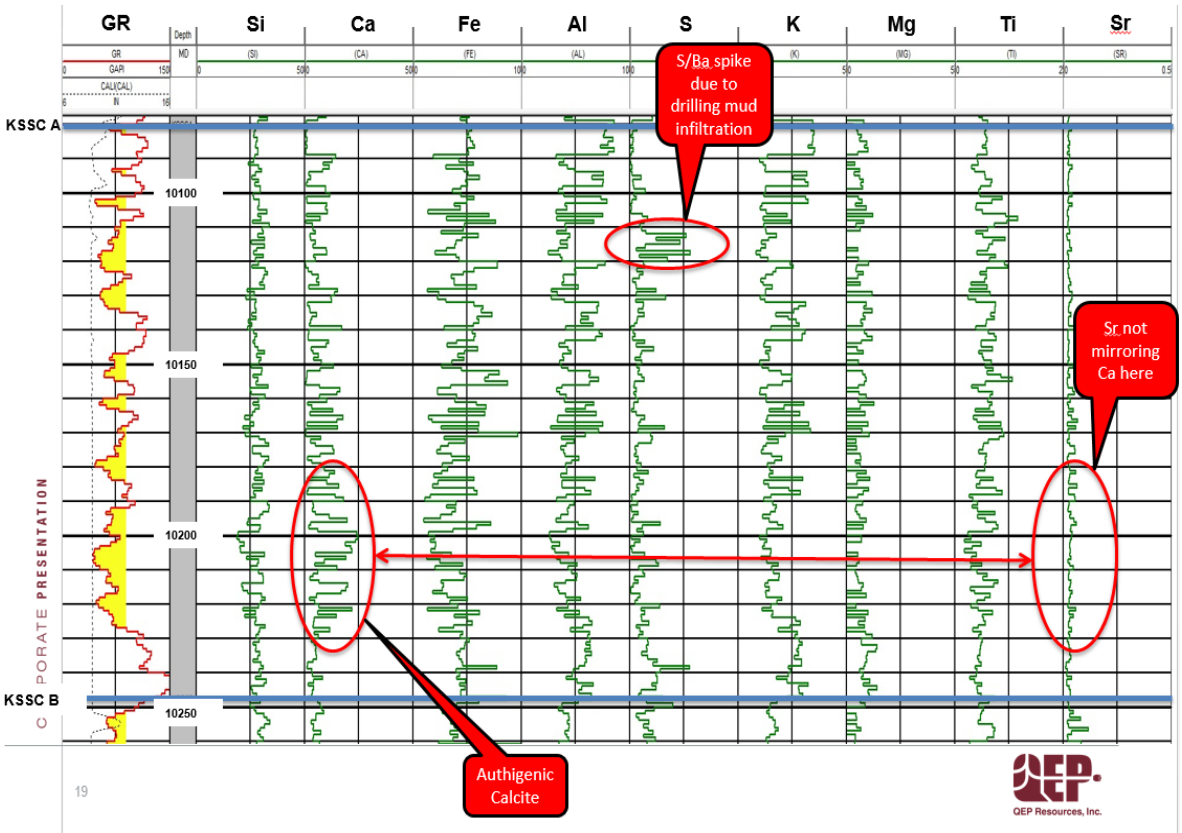

Figure 14: XRF major elemental data displayed alongside gamma ray readouts in the Kansas City "A" formation.

KANSAS CITY "D"

An interpretation of the Kansas City "D" formation suggests the presence of chlorite coating the pore spaces in Figure 15. This iron-rich cement is interpreted from the high intensity of the Fe log and without the corresponding spike in sulfur as well effectively rules out pyrite. Knowing exactly how much chlorite cement is present would require further XRD and SEM testing to be done. Another possibility would be the presence of siderite ($FeCO_3$) in this section, which was confirmed in person in the cored interval.

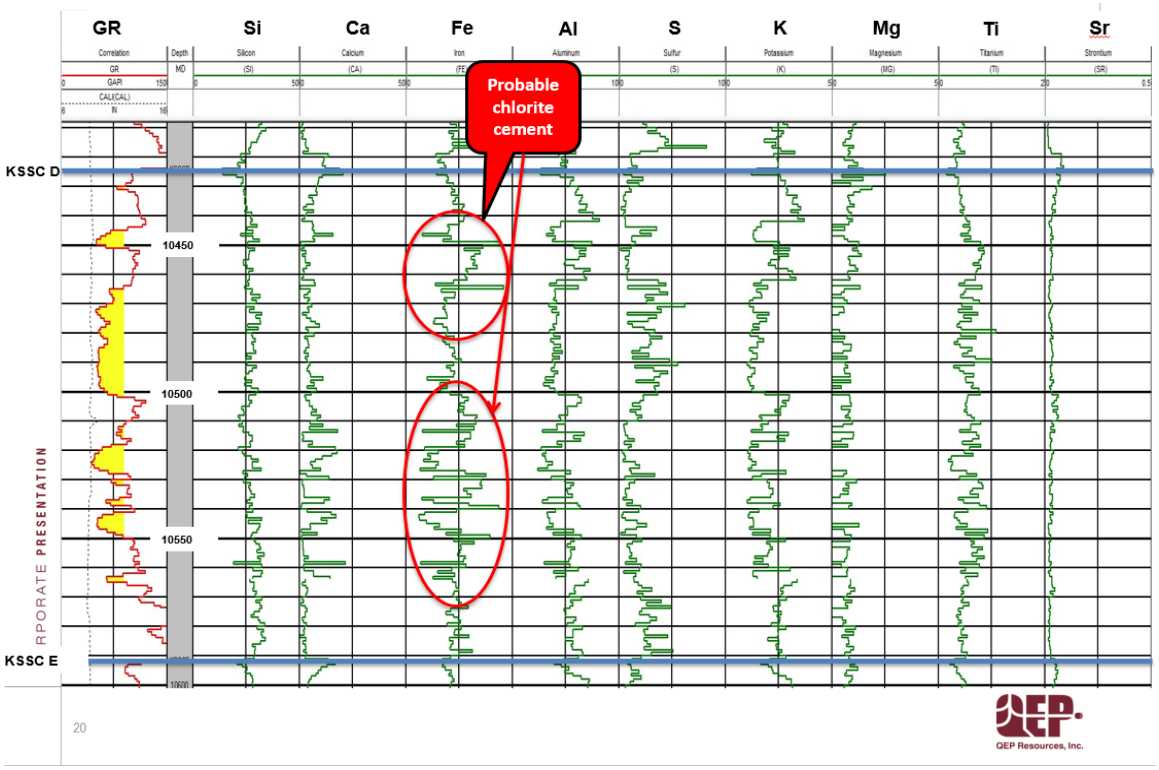

Figure 15: XRF major elemental data displayed alongside gamma ray readouts in the Kansas City "D" formation.

The organic indicators in the Kansas City “D” section in Figure 16 contain some well-defined increases in the organic indicating elements that is interpreted as another maximum flooding surface. There is also a distinct spike in the gamma ray which again confirms a solid potential source rock and an anoxic environment in which these sediments were deposited.

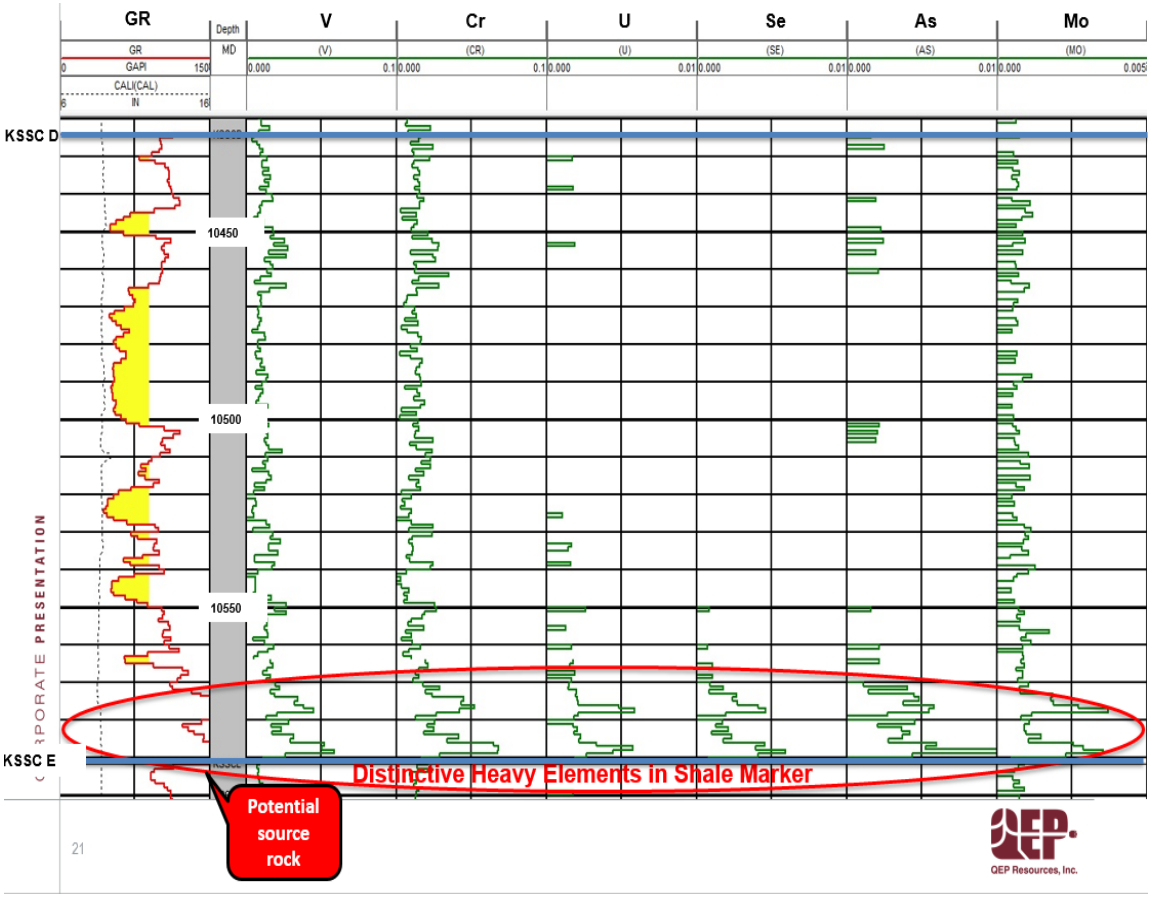

Figure 16: XRF heavy elemental data being shown alongside the gamma ray readout in the Kansas City “D” formation.

Fe/S and Al vs. K Plots

INTRODUCTION

Major element plots can help define mineralogy of a formation by showing their elemental abundance. For example, the presence of pyrite can be interpreted by looking at a curve with sulfur and iron and examining their relationship and correlation. Likewise, comparing aluminum and potassium is an excellent gauge for clay content in the formation.

RESULTS

In Figure 17 on the left, trending data points increasing linearly in this manner indicates pyrite and on the right of the figure we have differing trend lines indicating clay content. The data were rearranged in Microsoft Excel and plots were made for each different well in the study to show trends of these major elements.

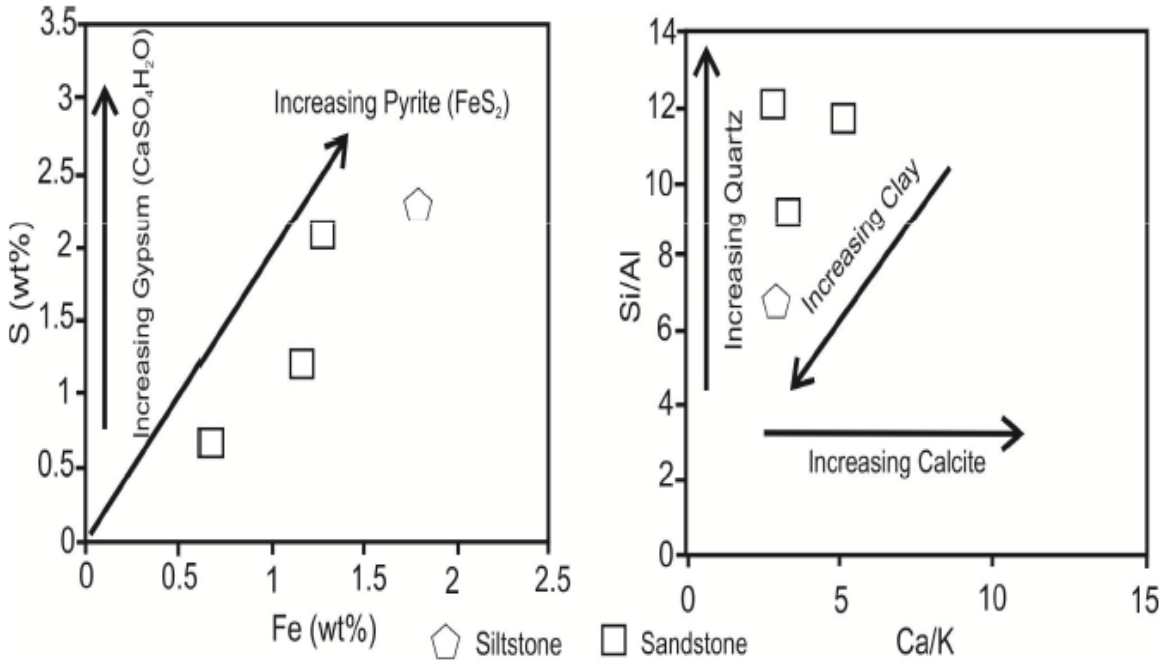

Figure 17: Iron and sulfur plots shown indicating trends of pyrite as well as Si/Al vs. Ca/K displaying trends of clay and calcite (Somarin 2010).

In figure 18 the iron and sulfur plots display each section of the stratigraphy starting with the Lansing section. In this area there is very little, if any, pyrite. In the Kansas City formations (Figures 18 & 19) more pyrite is appearing and the trend is beginning to be broken of mainly iron rich lithology. The Kansas City "D" formation displays the most pyritic parts of the stratigraphy. The Caldwell, Cherokee, and Granite Wash "A" formations (Figure 20) show the composition in this area is predominantly iron rich and suggests chlorite in these formations. This was confirmed with the supplemental SEM work done on the core that there was indeed 19.3% authigenic chlorite cement in the Granite Wash formation of one of the wells.

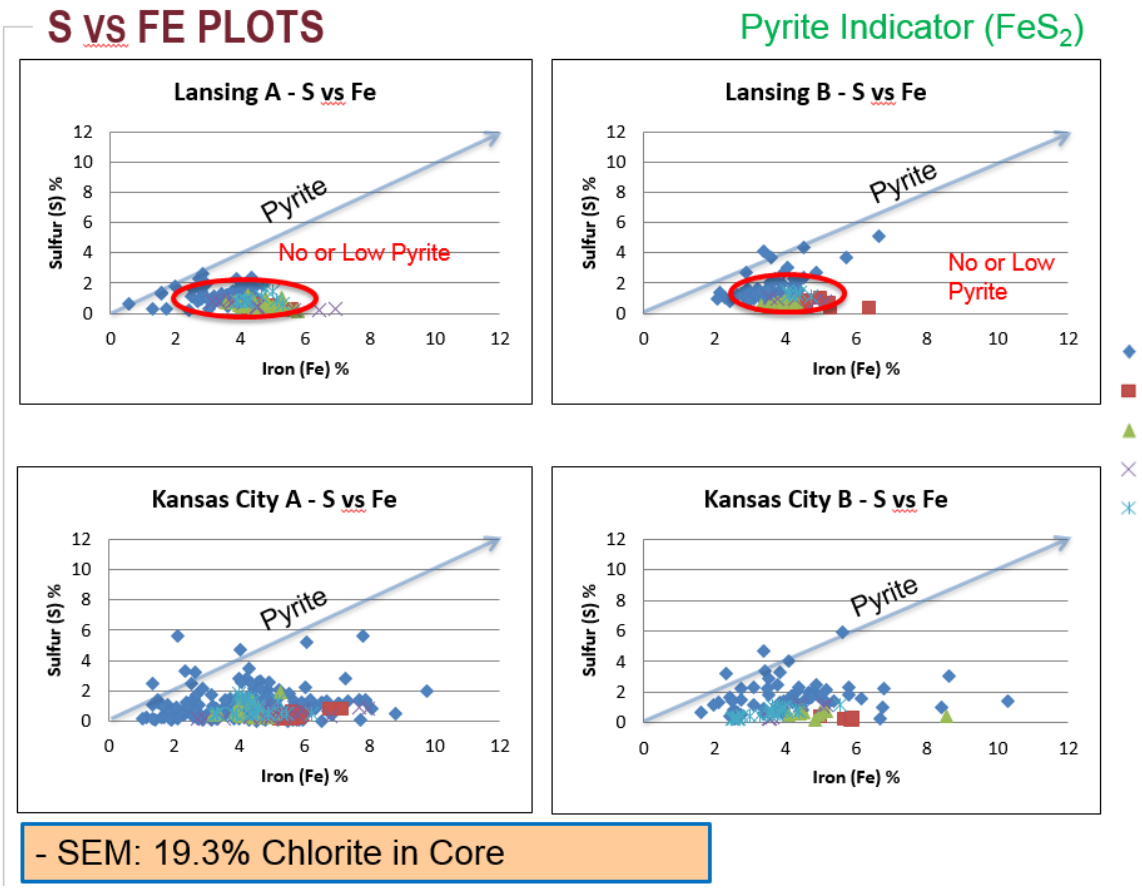

Figure 18: Sulfur and iron plots displaying pyrite and chlorite content covering Lansing and Kansas City "A" and "B" formations over all wells in the study.

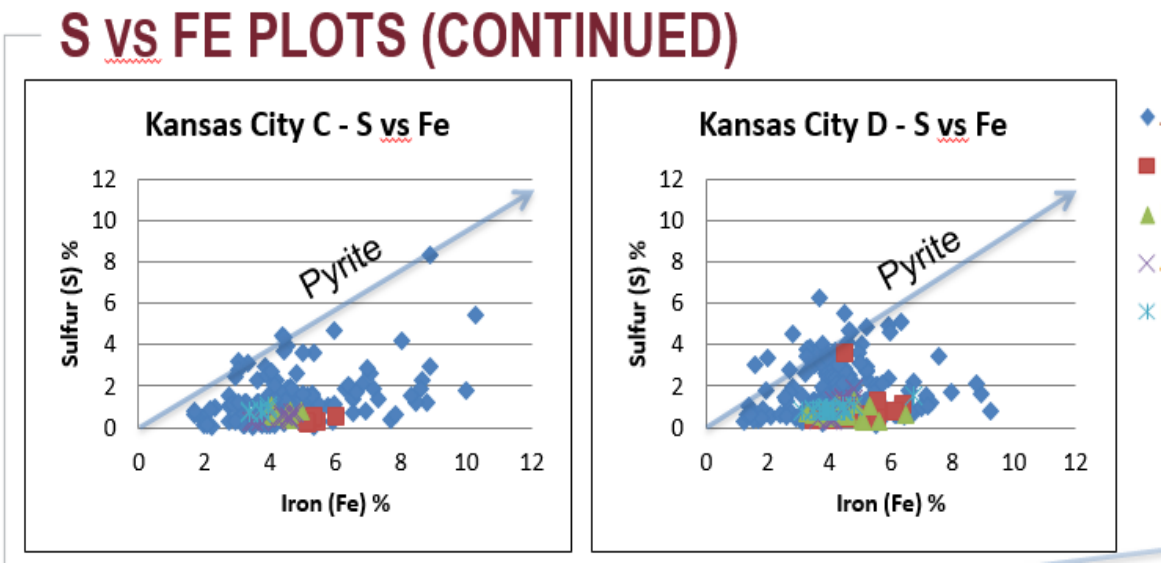

Figure 19: Sulfur and iron plots displaying pyrite and chlorite content covering Kansas City "C" and "D" formations over all wells in the study.

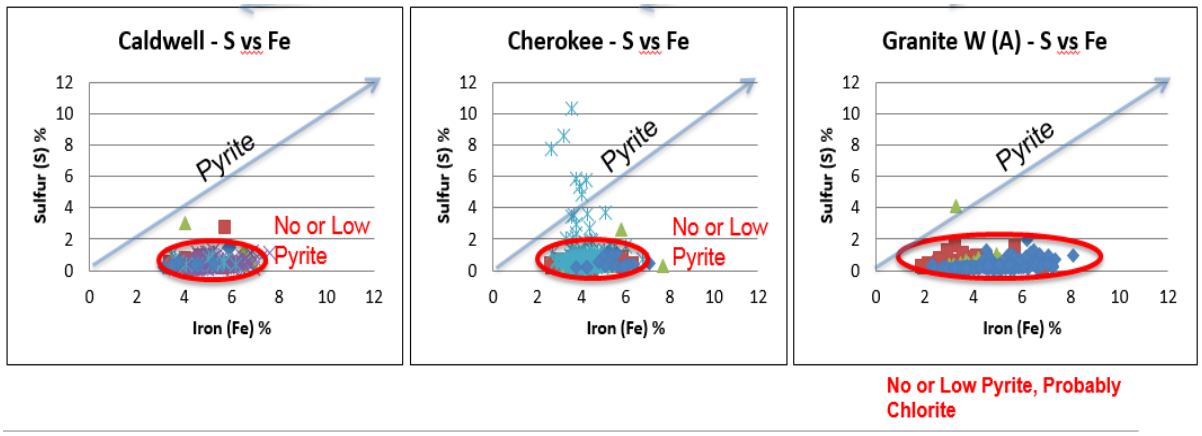

Figure 20: Sulfur and iron plot displaying pyrite and chlorite content covering the Caldwell, Cherokee, and Granite Wash "A" formations over all wells in the study.

The photograph taken, in Figure 21, with the scanning electron microscope shows the authigenic chlorite cement coating potassium-feldspar grains in an arkosic sandstone. This is confirmation that the XRF data are conclusive in showing this cement in the major elemental data. The occurrence of chlorite cement is detrimental because it is acid sensitive and can produce an iron-rich gel that can clog the pore throats and reduce permeability.

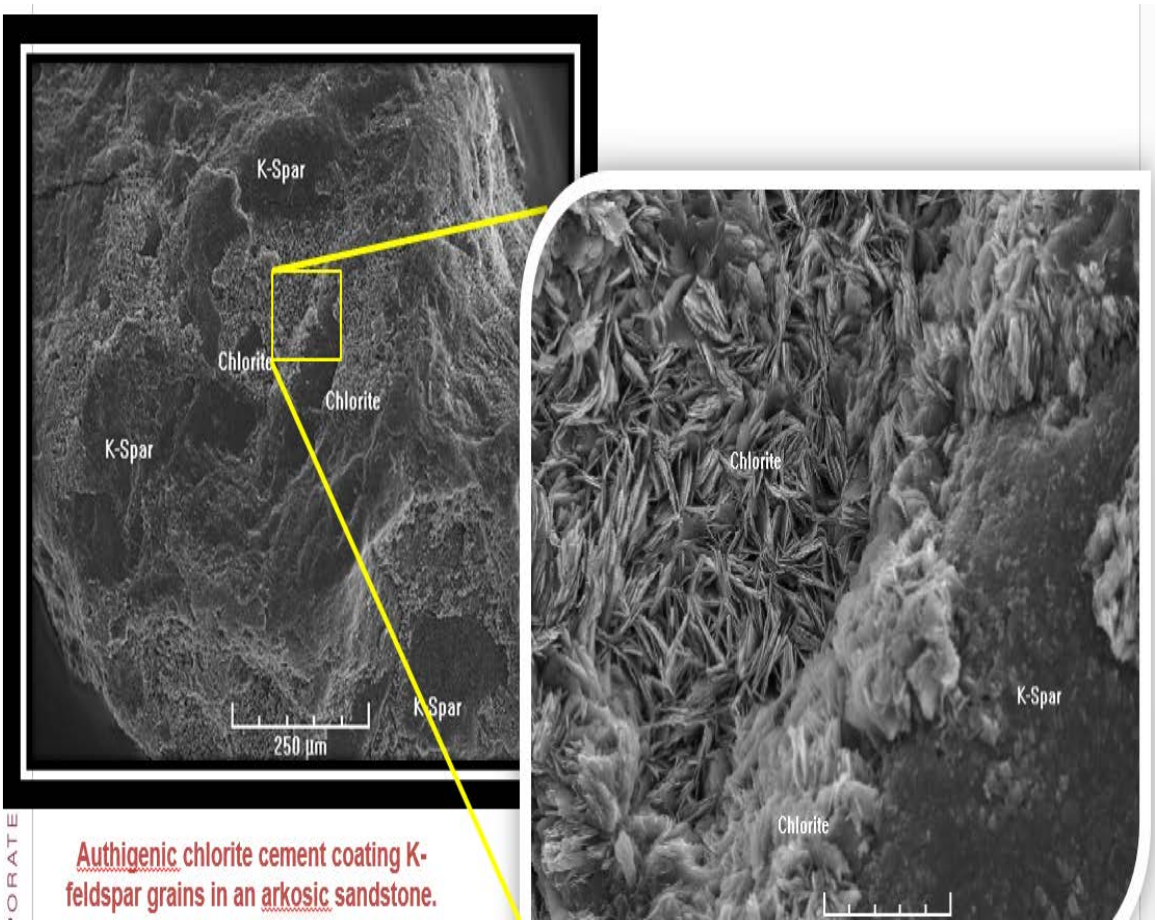

Figure 21: Scanning electron microscope (SEM) photograph of authigenic chlorite cement coating potassium-feldspar grains in an arkosic sandstone

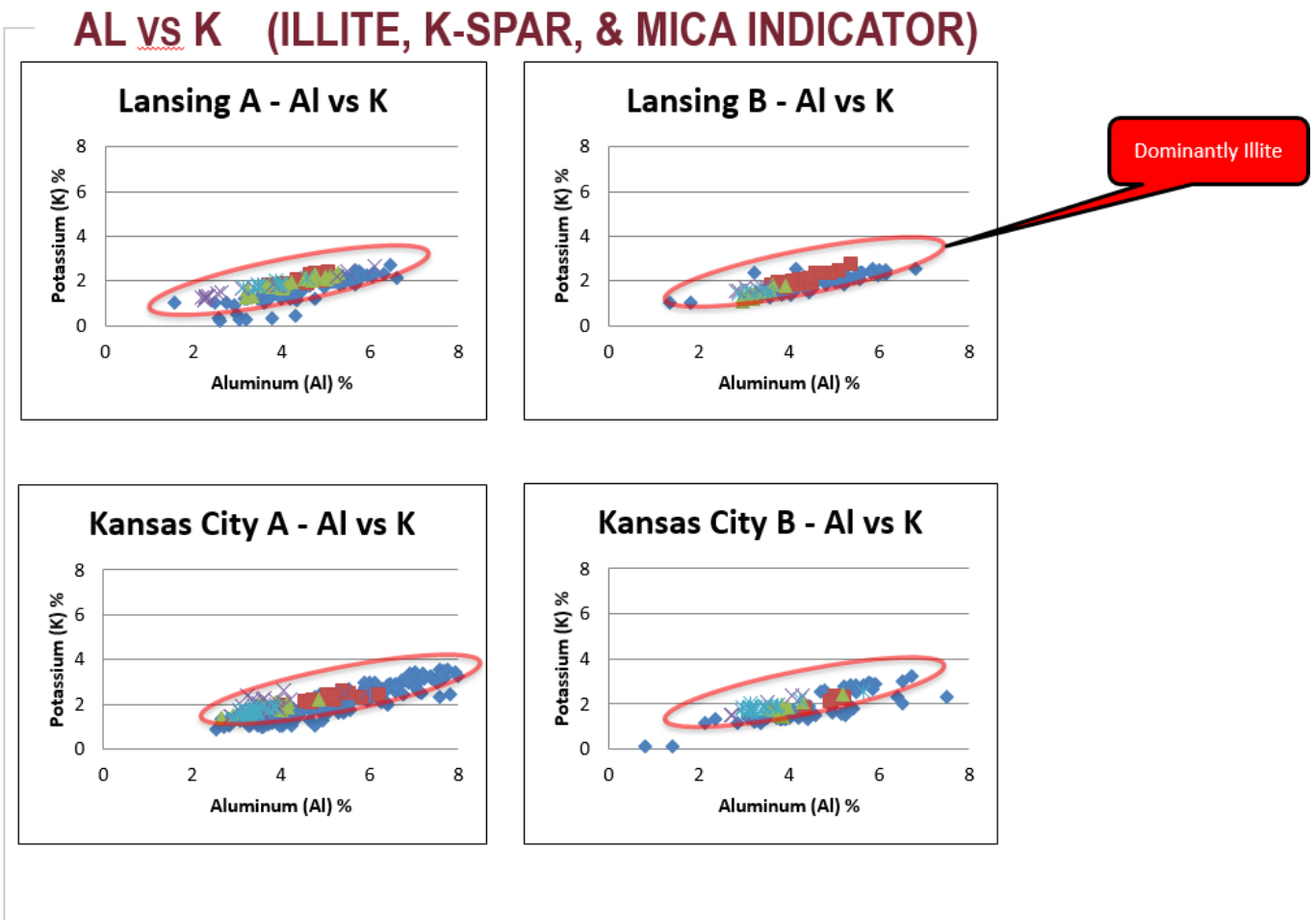

Figure 22: Aluminum and potassium plots displaying clay content in the Lansing and Kansas City "A" and "B" formations in all wells.

In figures 22 and 23 the clay plots of aluminum versus potassium are displayed. Making an assessment of all of the data collectively through all of the formations of the study there is a very strong trend. Aluminum-rich illite is the main rock type that is being shown by the data in all formations. Clays and mudstones can have a major effect and tend not to have high porosities and permeabilities. The lack of brittleness as well can be a troubling factor when trying to fracture the rock during production.

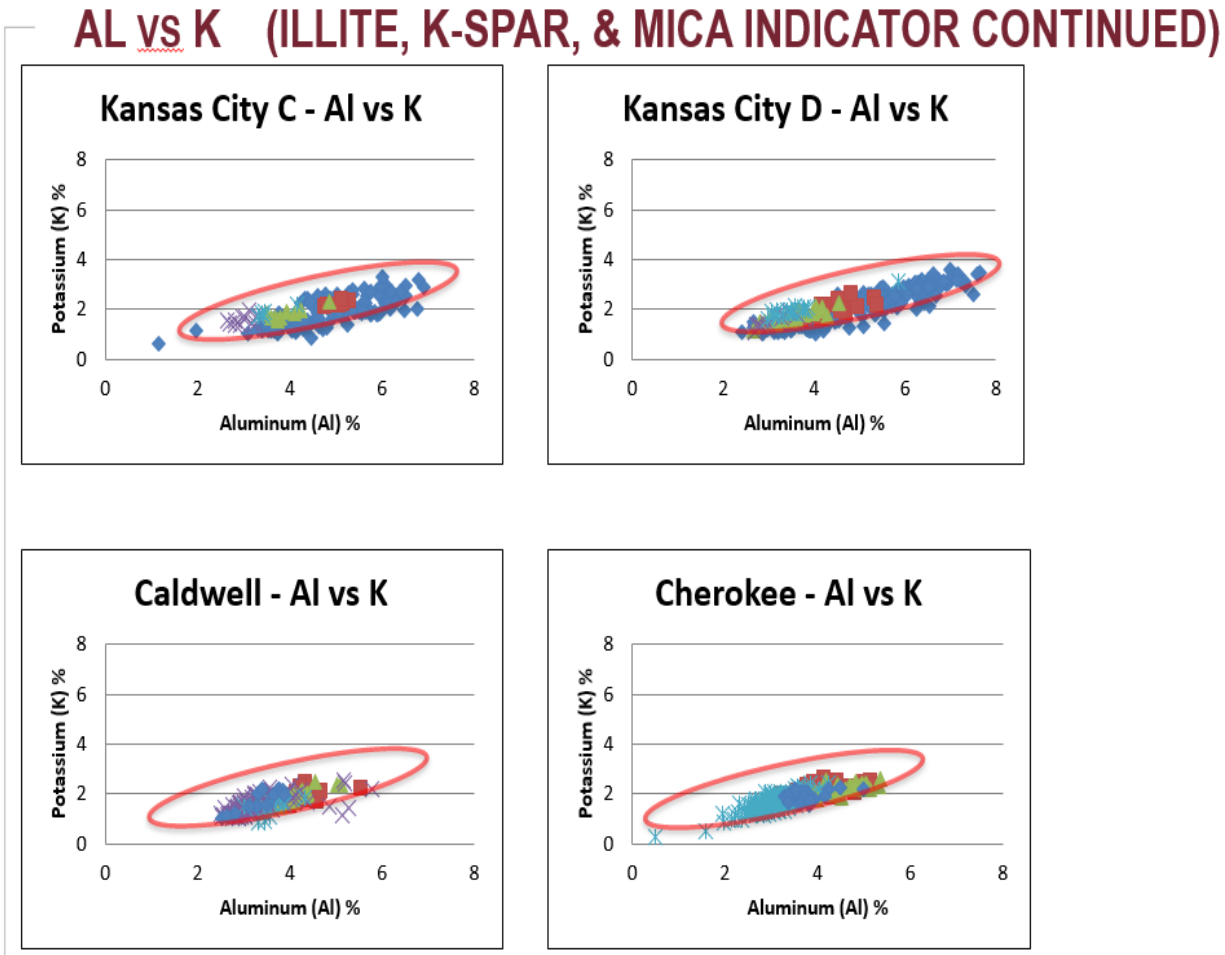

Figure 23: Aluminum and potassium plots displaying clay content in the Kansas City "C" and "D," Caldwell and Cherokee formations in all wells.

Rockview Data Results

In an effort to show how similar tools compare with the XRF data, an assessment and comparison with BakerHughes Rockview elemental spectroscopy testing is compared with the same XRF data. This Rockview data acquires geochemical data using elemental spectroscopy wireline logging tools. It provides accurate mineralogical characterizations

of the tested reservoir while reducing the uncertainty in interpretations that do not take into account mineralogical data (BakerHughes). In Figure 24, we have displayed the major elements that both devices detect and can make the observation that they are very similar. Furthermore, the accuracy of the elemental data in modeling mineralogy and lithology is comparable with XRD analyses (Marsala et al., 2011). The less expensive XRF device is able to read the elemental composition of the rocks and do so with similar results with more advanced and costly technology.

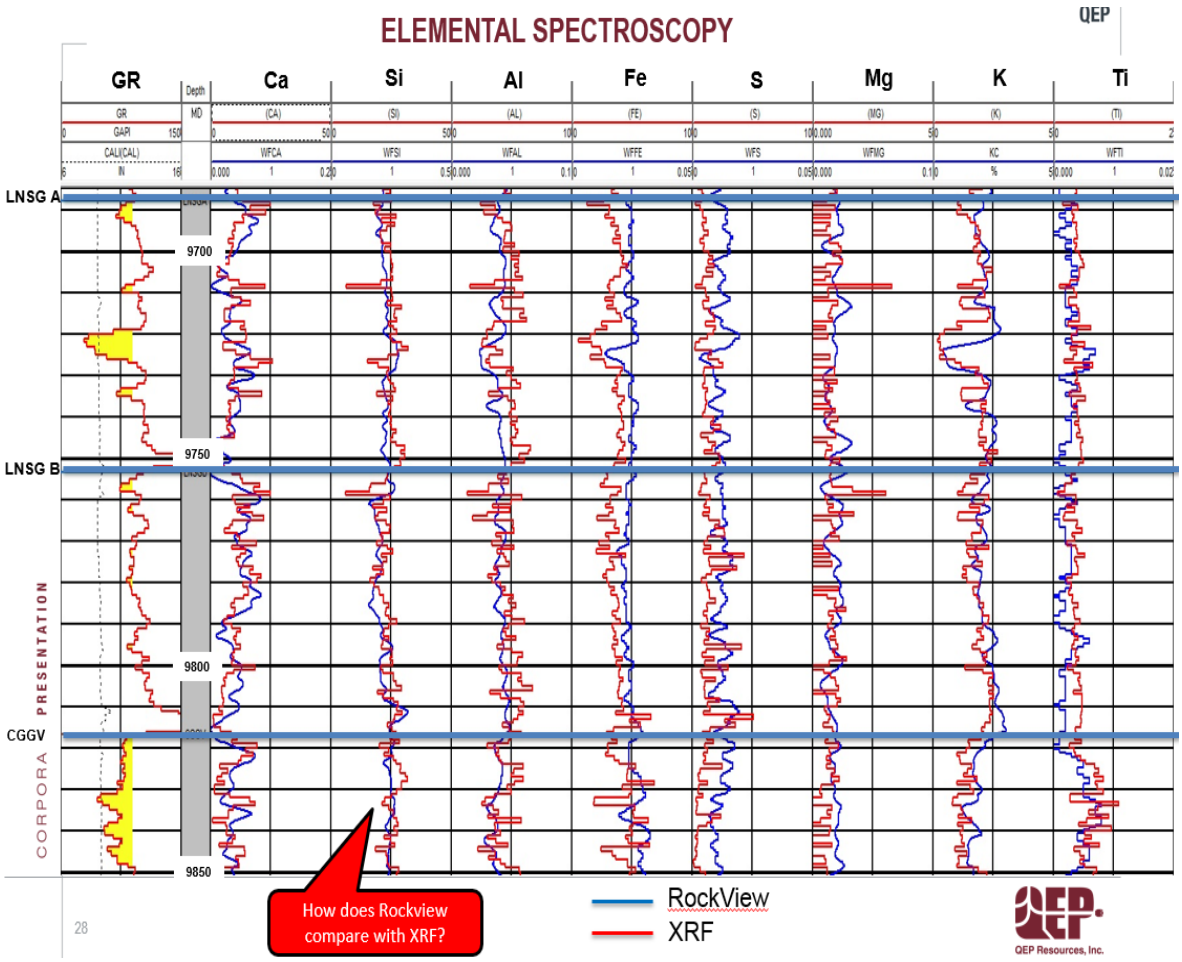

Figure 24: XRF data superimposed onto BakerHughes' Rockview nuclear magnetic resonance elemental spectroscopy data to show similar results from the XRF device.

Chapter 5 Conclusions and Future Work

OVERVIEW

X-ray Fluorescent technology is a viable and convenient supplemental tool in helping define reservoir characteristics of oil and gas bearing reservoirs. It can serve as a preliminary method to analyze hydrocarbon bearing rocks and the usefulness of this technology lies in understanding the elemental makeup of rock samples at its very basic level. With this study of the Granite Wash area using the XRF device, it is demonstrated that this method can be used effectively to determine rock type, pore cement presence, and clay content; all of which contribute to reservoir characterization and petrophysical properties. While it is difficult to find substitutions for core samples, NMR, XRD, and SEM tests, the XRF device offers similar data with the caveat of more user interpretation to complement the necessary reservoir characteristics. Moreover, potential interpretation of sequence stratigraphic maximum flooding surfaces can also be pointed out by geologists. The technology behind the XRF instrument, methodology, and geologic setting of the Granite Wash are all examined in detail in this study. While this technology is valid currently in the oil and gas industry, more advancement in the depth of analysis offered by the XRF instrument can be researched further to offer more insight.

References

Algeo, Thomas J., and Harry Rowe. "Paleoceanographic Applications of Trace-metal Concentration Data." *Chemical Geology* 324-325 (2012): 6-18. Print.

Algeo, Thomas J., and Timothy W. Lyons. "Mo–total Organic Carbon Covariation in Modern Anoxic Marine Environments: Implications for Analysis of Paleoredox and Paleohydrographic Conditions." *Paleoceanography* 21.1 (2006). Print

Aplin, Andrew C., and Joe H. S. Macquaker. "Mudstone Diversity: Origin and Implications for Source, Seal, and Reservoir Properties in Petroleum Systems." *AAPG Bulletin* 95.12 (2011): 2031-059. Print.

Ball, Mahlon M., Mitchell E. Henry, and Sherwood E. Frezon. "Petroleum Geology of the Anadarko Basin Region, Province (115), Kansas, Oklahoma, and Texas." Department of the Interior U.S. Geological Survey, 1991. Web. 1 May 2014.

De Villiers, Stephanie. "Seawater Strontium and Sr/Ca Variability in the Atlantic and Pacific Oceans." *Earth and Planetary Science Letters* 171.4 (1999): 623-34. *ELSEVIER*. Web. 1 May 2014.

Dutton, Shirley P., and Lynton S. Land. "Meteoric Burial Diagenesis of Pennsylvanian Arkosic Sandstones, Southwestern Anadarko Basin, Texas." *AAPG Bulletin* 69.1 (1985): 22-38. Print.

Dutton, Shirley P. "Pennsylvanian Fan-Delta and Carbonate Deposition, Mobeetie Field, Texas Panhandle." *AAPG Bulletin* 66.4 (1982): 389-407. Print.

Fitton, G., 1997. X-Ray fluorescence spectrometry. in: Gill, R. (Ed.), Modern Analytical Geochemistry: An Introduction to Quantitative Chemical Analysis for Earth, Environmental and Material Scientists. Addison Wesley Longman, Harlow, England. pp. 87-115.

"GEO ExPro - Unique and Fast Analysis in the Field." *GEO ExPro - Unique and Fast Analysis in the Field*. Web. 25 Apr. 2014.

"Granite Wash Information." *Granite Wash for RRC*. Web. 01 May 2014.

Marsala, A.F., T. Loermans, S. Shen, C. Scheibe, and R. Zereik. "Portable Energy-Dispersive X-Ray Fluorescence Integrates Mineralogy And Chemostratigraphy Into Real-Time Formation Evaluation." *OnePetro*. Society of Petrophysicists and Well Log Analysts, 2011. Web. 01 May 2014.

"Maximum Flooding Surface." *Schlumberger Oilfield Glossary*. Web. 01 May 2014.

Meunier, J. D. "The Composition and Origin of Vanadium-Rich Clay Minerals in Colorado Plateau Jurassic Sandstones." *Clays and Clay Minerals* 42.4 (1994): 391-401. Print.

Mitchell, John. "Horizontal Drilling of Deep Granite Wash Reservoirs, Anadarko Basin, Oklahoma and Texas." *Shale Shaker: The Journal of the Oklahoma City Geological Society* 62.2 (2011): 118-67. Print.

"Petrology and Mineralogy." *Core Laboratories:*. Web. 25 Apr. 2014.

"Portable XRF Analyzer & Price List." *Mining Examiner*. Web. 25 Apr. 2014.

"RockView Service." *Home*. BakerHughes. Web. 25 Apr. 2014.

Ross, D.J.K., and Bustin, R.M., 2009, Investigating the use of sedimentary geochemical proxies for paleoenvironment interpretation of thermally mature organic-rich strata—Examples from the Devonian-Mississippian shales, western Canadian sedimentary basin: Chemical Geology, v.260, p. 1-19.

"Routine Rock Properties." *Core Laboratories: Spectral Core Gamma System*. Web. 01 May 2014.

Rowe, Harry, Niki Hughes, and Krystin Robinson. "The Quantification and Application of Handheld Energy-dispersive X-ray Fluorescence (ED-XRF) in Mudrock Chemostratigraphy and Geochemistry." *Chemical Geology* 324-325 (2012): 122-31. Print.

Smith, Christopher N., and Ariel Malicse. "Rapid Handheld X-ray Fluorescence (HHXRF) Analysis of Gas Shales." *AAPG Datapages*. Web.

"Spectral Gamma Ray (CSNG™) Log Service." *Halliburton*. Web. 01 May 2014.

ThermoScientific. "Upstream Exploration and Production with the Thermo Scientific Niton XL3t 900 GOLDD Series XRF Analyzer." *Niton*. ThermoScientific, 2010. Web. 25 Apr. 2014.

"UGA Stratigraphy Lab." *An Online Guide to Sequence Stratigraphy*. Web. 01 May 2014.

"XRF Glossary - What Is XRF Technology - Thermo Scientific." *XRF Glossary - What Is XRF Technology - Thermo Scientific*. Web. 25 Apr. 2014.